

MODIFIED GRADIENT APPROACH
TO A TIME OPTIMAL CONTROL PROBLEM

A Thesis
Presented to
the Faculty of Graduate Studies and Research
University of Manitoba

In Partial Fulfillment
of the Requirements for the Degree
Master of Science in Electrical Engineering

by
Harold G. Elders
May 1971



ABSTRACT

This thesis is concerned with the application of time optimal theory, utilizing Pontryagin's Maximum Principle, to the problem of synchronous machine stability. The plant is the Heffron and Phillips model of a synchronous generator. The troublesome two - point boundary value problem, which is always associated with the maximum principle, regardless of the plant, is solved by an iterative scheme simulated on a hybrid computer. It is shown that an optimal bang bang signal, applied to the exciter of a synchronous generator connected to an infinite bus, greatly improves the stability of the system.

ACKNOWLEDGEMENT

The author wishes to express his appreciation to his thesis advisor, Professor W.H. Lehn, for suggesting the topic, as well as for his guidance during the past year. Thanks are also extended to Professor G.W. Swift for his discussions concerning the thesis topic.

The financial assistance from Manitoba Hydro, which permitted this work to be carried out, is also acknowledged.

TABLE OF CONTENTS

	PAGE
ABSTRACT	ii
ACKNOWLEDGEMENT	iii
LIST OF ILLUSTRATIONS	v
CHAPTER	
I. INTRODUCTION	1
II. OPTIMAL CONTROL THEORY	4
III. MODIFIED GRADIENT METHOD AND THE ITERATIVE SCHEME	10
IV. HYBRID COMPUTER PROGRAM	15
V. EXPERIMENTAL RESULTS	22
VI. CONCLUSIONS AND SUGGESTIONS FOR FURTHER STUDY	51
APPENDIX	
A. COMPUTER SYMBOLS	53
POT SETTINGS	57
INITIAL SETTINGS	57
BIBLIOGRAPHY	58

LIST OF ILLUSTRATIONS

FIGURE	PAGE
1. Block diagram of the Heffron and Phillips model of a synchronous generator	5
2. Control function $u(t)$	8
3. Block diagram of the iterative scheme	11
4. Control functions $u_m(t)$	13
5. Analog Computer Program	16
6. Mechanical torque input disturbances	21
7. $\Delta\dot{\delta}$ versus $\Delta\delta$ showing optimal switching curves (a;b) for various torque input magnitudes (c = .07, d = .096, e = .12) (constant control magnitude)	24
8. $\Delta\psi_{fd}$ versus $\Delta\delta$ showing optimal switching curves (a;b) for various torque input magnitudes (c = .07, d = .096, e = .12) (constant control magnitude)	25
9. $\Delta\psi_{fd}$ versus $\Delta\dot{\delta}$ showing optimal switching curves (a;b) for various torque input magnitudes (c = .07, d = .096, e = .12) (constant control magnitude)	26
10. Dynamic stability of $\Delta\dot{\delta}$ and $\Delta\delta$ with time optimal control. Constant disturbance input magnitude (0.1). Variable control magnitude (a = 0.07, b = 0.06, c = 0.042)	29

11.	Relationship between control and input magnitude yielding time optimal control	30
12.	Time optimal solution of $\Delta\dot{\delta}$ and $\Delta\delta$, input magnitude a)0.033 b)0.066 c)0.099 d)0.132	32
13.	Time optimal solution of $\Delta\psi_{fd}$ and Δv_t , input magnitude a)0.033 b)0.066 c)0.099 d)0.132	33
14.	Time optimal trajectories in the $\Delta\dot{\delta}$ versus $\Delta\delta$ plane, input magnitudes a)0.033 b)0.066 c)0.099 d)0.132, control magnitudes a)0.02 b) 0.04 c)0.06 d)0.08	34
15.	Time optimal trajectories in the $\Delta\psi_{fd}$ versus $\Delta\delta$ plane, input magnitudes a)0.033 b)0.066 c)0.099 d)0.132, control magnitudes a)0.02 b)0.04 c)0.06 d)0.08	35
16.	Time optimal trajectories in the $\Delta\psi_{fd}$ versus $\Delta\dot{\delta}$ plane, input magnitudes a)0.033 b)0.066 c)0.099 d)0.132, control magnitudes a)0.02 b)0.04 c)0.06 d)0.08	36
17.	Steps in iterative scheme.	38
18.	Dynamic stability of $\Delta\dot{\delta}$ and $\Delta\delta$, with no control (a) and with optimal control (b)	40
19.	Dynamic stability of ΔP_a , $\Delta\psi_{fd}$ and Δv_t , with no control (a) and with optimal control (b)	41

FIGURE

PAGE

20.	Experimental results from an M.Sc.EE thesis presented by G.W. Ryckman ²⁰	42
21.	$\Delta \dot{\delta}$ versus $\Delta \delta$ phase plane plot for a)Uncompensated case b)Time - optimal case a')Uncompensated case c)Sub - optimal case . . .	44
22.	Dynamic stability of $\Delta \dot{\delta}$ and $\Delta \delta$ with no control (a) and with time optimal control (b)	45
23.	Dynamic stability of ΔP_a and Δv_t with no control (a) and with time optimal control (b)	46
24.	Dynamic stability of $\Delta \dot{\delta}$, $\Delta \delta$, and ΔP_a with no control (a) and with sub - optimal control (b) .	47

CHAPTER I

INTRODUCTION

In the past ten years, increasing attention has been focused on the application of excitation control to the behavior of the torque angle and speed, of a synchronous generator, following a disturbance, such as a mechanical torque disturbance. Many theoretical results have been published in the area of system optimization, and except for a few exceptions have mainly dealt with low-order systems. One of the notable exceptions has been a paper by Fred B. Smith²¹, who presented a method for obtaining a forcing function, $u(t)$, as a function of the state variables, without requiring use of the phase space concept. An iterative procedure which relies on the connection between the adjoint system and the time optimal control function, was applied to a fourth order system by H. K. Knudsen¹². Using a cost functional, Yao - Nan Yu²⁴ has applied control theory to improve the dynamic response of a power system. G. A. Korn and H. Kosako¹⁴ have attacked the problem of functional optimization using the so called random - perturbation method. This method consists of adding a random perturbation $\Delta u(t)$ to $u(t)$, computing the given criterion function on an analog computer, and comparing it with the value of the criterion function

calculated, with no perturbation on $u(t)$. If an improvement has been made, the new value $u(t) + \Delta u(t)$ is stored and the process repeated.

Optimal control theory, as has been shown in the past, can be successfully applied to the power system field. Using a modified gradient approach an iterative scheme was built on a hybrid computer to solve the problem of power system damping. In order to test the method, a second order system ($\frac{1}{s^2}$), and a third order system ($\frac{1}{s^2(s+1)}$), were simulated and the time optimal control solutions were found. Variations in the initial conditions of the adjoint variables were used. The results for both systems agreed very well with theory; although for the third order plant the adjoint system was very sensitive to changes in the adjoint initial conditions and great care had to be taken to prevent saturation of the computer.

The fourth order system simulated was the Heffron and Phillips model of a four kilovolt-amperes wye-connected synchronous generator attached to an infinite bus through external reactance. All data dealing with the synchronous generator have been taken from an M. Sc. thesis, completed at the University of Manitoba in 1970, by Gordon W. Ryckman²⁰. After simulation of the adjoint system for the fourth order plant it was found to be far too sensitive to parameter changes,

and therefore could not be used satisfactorily in the program.

As an alternative scheme the adjoint system method was not used, and instead the control function, $u(t)$, was built with adjustable switching times (t_x). To obtain a successively improved control function $u(t)$, the switching times t_x are each perturbed by Δt_x , and the criterion function, which in this case is the minimum time T , is calculated. If $T(t_x + \Delta t_x)$ is less than $T(t_x)$, the value of $u(t)$ with the new switching times $t_x + \Delta t_x$ is stored and the process is continued until the function $u(t)$ producing the minimum time T is found.

All values given in the thesis are in per unit (pu.), with the base quantities being the rated values of torque angle, speed, field voltage, field flux and accelerating power.

CHAPTER II

OPTIMAL CONTROL THEORY

Optimal control theory has been covered thoroughly by many authors, and therefore, only the fundamentals as applied to the particular problem, concerning power system damping, will be discussed here. A block diagram of the Heffron and Phillips model, used to represent a synchronous generator connected to an infinite bus, is shown in Figure 1. The state variables for the system are the change in torque angle ($\Delta\delta$), the change in speed ($\Delta\dot{\delta} = \eta$), the change in field flux ($\Delta\psi_{fd}$), and the change in field voltage (ΔE_{fd}). The control $u(t)$ is the input signal to the static exciter, represented in the block diagram by the transfer function $\frac{-K_e}{1 + sT_e}$. The synchronous machine and controller equations

are written in the form $\dot{X} = AX + Bu$:

$$\begin{bmatrix} \Delta\dot{\delta} \\ \dot{\eta} \\ \Delta\dot{\psi}_{fd} \\ \Delta\dot{E}_{fd} \end{bmatrix} = \begin{bmatrix} 0 & 1 & 0 & 0 \\ \frac{-K_1}{M} & \frac{-D}{M} & \frac{-K_2}{M} & 0 \\ \frac{-K_4}{K_3 T'_{do}} & 0 & \frac{-1}{K_3 T'_{do}} & \frac{1}{T'_{do}} \\ 0 & 0 & 0 & \frac{-1}{T_e} \end{bmatrix} \begin{bmatrix} \Delta\delta \\ \eta \\ \Delta\psi_{fd} \\ \Delta E_{fd} \end{bmatrix} + \begin{bmatrix} 0 \\ 0 \\ 0 \\ \frac{-K_e}{T_e} \end{bmatrix} (u) + \begin{bmatrix} 0 \\ \frac{\Delta P_M}{M} \\ 0 \\ 0 \end{bmatrix} \quad \text{---II-I}$$

A time functional $J = T = \int_0^t dt$ is chosen and Pontryagin's

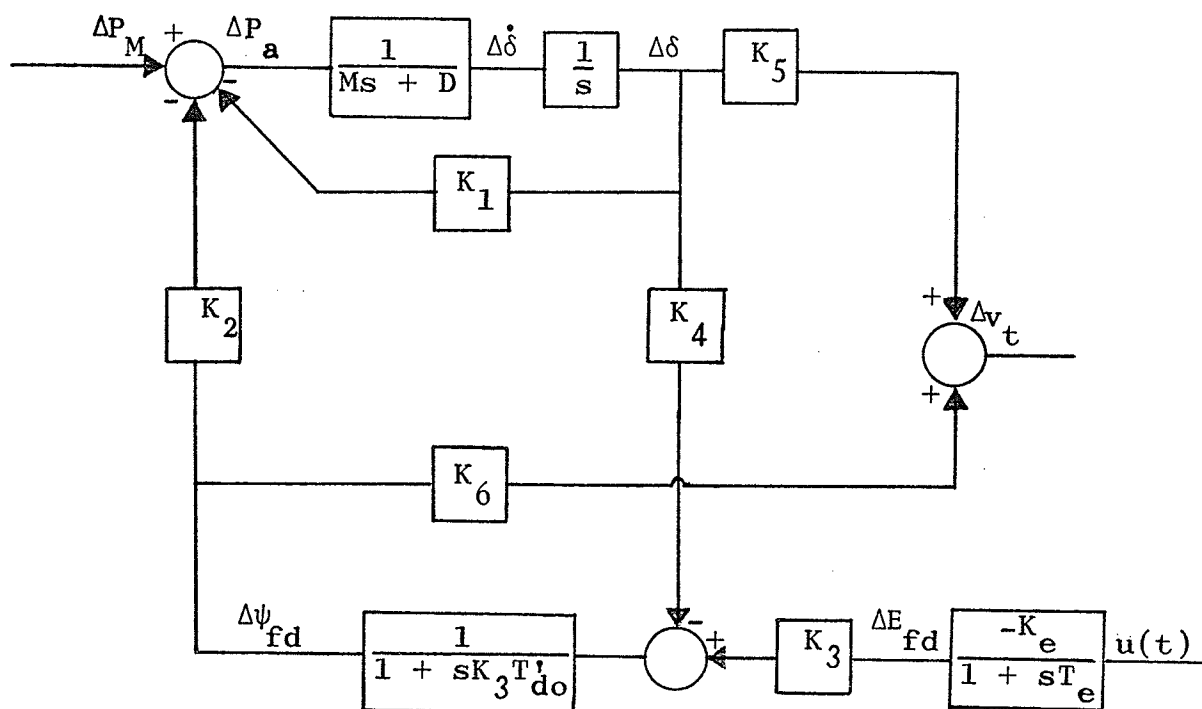


Figure 1.* Block diagram of the Heffron and Phillips model of a synchronous generator.

* An extract from the M.Sc.EE thesis presented by G.W. Ryckman²⁰.

maximum principle¹¹ is applied to find the optimal control function $u(t)$, which minimizes the functional. The solution of the problem begins with the introduction of the adjoint vector, ψ , and a Hamiltonian function H , of the following form:

$$\begin{aligned}
 H &= -1 + \psi^T A X + \psi^T B U \\
 &= -1 + \psi_1(\eta) + \psi_2 \left(-\frac{K_1}{M} \Delta \delta - \frac{D}{M} \eta - \frac{K_2}{M} \Delta \psi_{fd} \right) + \psi_3 \left(-\frac{K_4}{K_3 T_{do}} \Delta \delta \right. \\
 &\quad \left. - \frac{1}{K_3 T_{do}} \Delta \psi_{fd} + \frac{1}{T_{do}} \Delta E_{fd} \right) + \psi_4 \left(-\frac{1}{T_e} \Delta E_{fd} - \frac{K_e}{T_e} u \right)
 \end{aligned}
 \tag{II-2}$$

According to the maximum principle, in order for J to be minimized with respect to $u(t)$, H must be maximized by the proper choice of $u(t)$. For an optimal control function $u(t)$, ψ and X must be the solution of

$$\dot{X} = \frac{\partial H}{\partial \psi}, \quad \dot{\psi} = -\frac{\partial H}{\partial X}
 \tag{II-3}$$

The adjoint equations are of the form

$$\begin{bmatrix} \dot{\psi}_1 \\ \dot{\psi}_2 \\ \dot{\psi}_3 \\ \dot{\psi}_4 \end{bmatrix} = \begin{bmatrix} 0 & \frac{K_1}{M} & \frac{K_4}{K_3 T_{do}} & 0 \\ -1 & \frac{D}{M} & 0 & 0 \\ 0 & \frac{K_2}{M} & \frac{1}{K_3 T_{do}} & 0 \\ 0 & 0 & -\frac{1}{T_{do}} & \frac{1}{T_e} \end{bmatrix} \begin{bmatrix} \psi_1 \\ \psi_2 \\ \psi_3 \\ \psi_4 \end{bmatrix}
 \tag{II-4}$$

According to Pontryagin's maximum principle the control function is of the form

$$u(t) = U \operatorname{sgn}\left(-\frac{K_e}{T_e} \psi_4\right) \quad U = \text{a constant} \quad \text{---II-5}$$

where the switching instants are controlled by the adjoint variable ψ_4 .

A paper published by J. Grad and M. A. Brebner⁸, which finds all the eigenvalues of a real general matrix, was used to find the eigenvalues of the Heffron and Phillips plant. The system was found to have two real and two imaginary eigenvalues.* Because two of the eigenvalues are complex conjugates nothing can be said about the number of possible switching instants in the control $u(t)$. Due to the fact that the number of amplifiers is limited on the EAI** 580 hybrid computer, it was decided to solve for optimal solutions with a maximum of three switching instants t_1 to t_3 . At this time it should be noted that while the control function can have any number of switching instants, the control cannot remain forever and must, at time t_4 , be turned off.

*The values of K_1 to K_6 , M , D , T'_{do} , K_e and T_e are listed in Table 1.

**EAI - Electronic Associates, Inc.

The problem, therefore, is to determine the switching instants t_1 to t_4 as shown in Figure 2, which will maximize the Hamiltonian H and will yield the time optimal solution $u^*(t)$.

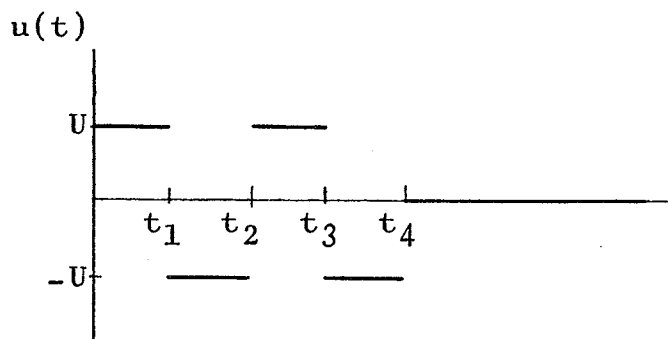


Figure 2.

As the final values of $\Delta\delta$ and $\Delta\psi_{fd}$ do not return to zero, but reach a constant level after a disturbance, the coordinates of both $\Delta\delta$ and $\Delta\psi_{fd}$ were shifted so that their final constant level was centered on the origin (see Figures 7,8,9,14,15,16,17,21). In this way each magnitude of disturbance input (N) can be looked on as a particular initial condition point in four dimensional state space. In state space, the problem can be viewed as one of bringing a point in four dimensional space to the origin in the shortest possible time, T . As has been mentioned in the Introduction the use of the adjoint system in the iterative scheme had to be abandoned. The adjoint system for a stable plant will

be unstable, and hence very sensitive to noise and parameter errors. On simulation of the adjoint system it was found that the switching instants were indeed far too sensitive to changes in the initial choice of adjoint variables. It was therefore decided to apply the modified gradient approach directly to the initial choice of switching instants t_1 to t_4 , rather than to the initial choice of the adjoint variables. One disadvantage to this approach is that simulation of the adjoint system requires fewer analogue components, than generation of the switching instants directly. As the number of analogue components is limited on the EAI 580 hybrid computer, the optimal solution for higher order plants can not be solved without a larger computer.

CHAPTER III

MODIFIED GRADIENT METHOD

and the ITERATIVE SCHEME

The modified gradient scheme works on the principle that changing each parameter t , by an amount proportional to the negative of its partial derivative $\frac{\partial T}{\partial t}$, will decrease the criterion function T . The parameters t_1 to t_4 are the switching instants of the function $u(t)$ and the time T is the criterion function $\int_0^t dt$ which has to be minimized. To best explain the modified gradient method, a block diagram of the iterative scheme is shown in Figure 3.

Initially the iterative scheme begins with the random choice of the control function $u_m(t)$ from Figure 4. The partial derivatives are calculated and during the update mode, $k(\frac{\partial T}{\partial t_x})$ is subtracted from the switching instants t_x . The constant k controls the speed of convergence. A small value of k , while approximating the steepest descent, makes for a slow convergence time. A reasonable convergence time for the iterative scheme is obtained by making a suitable choice for k , as well as by making continuous runs in the update mode as long as each value of T calculated is less than the previous value of T .

The partial derivatives are calculated using the central difference method:

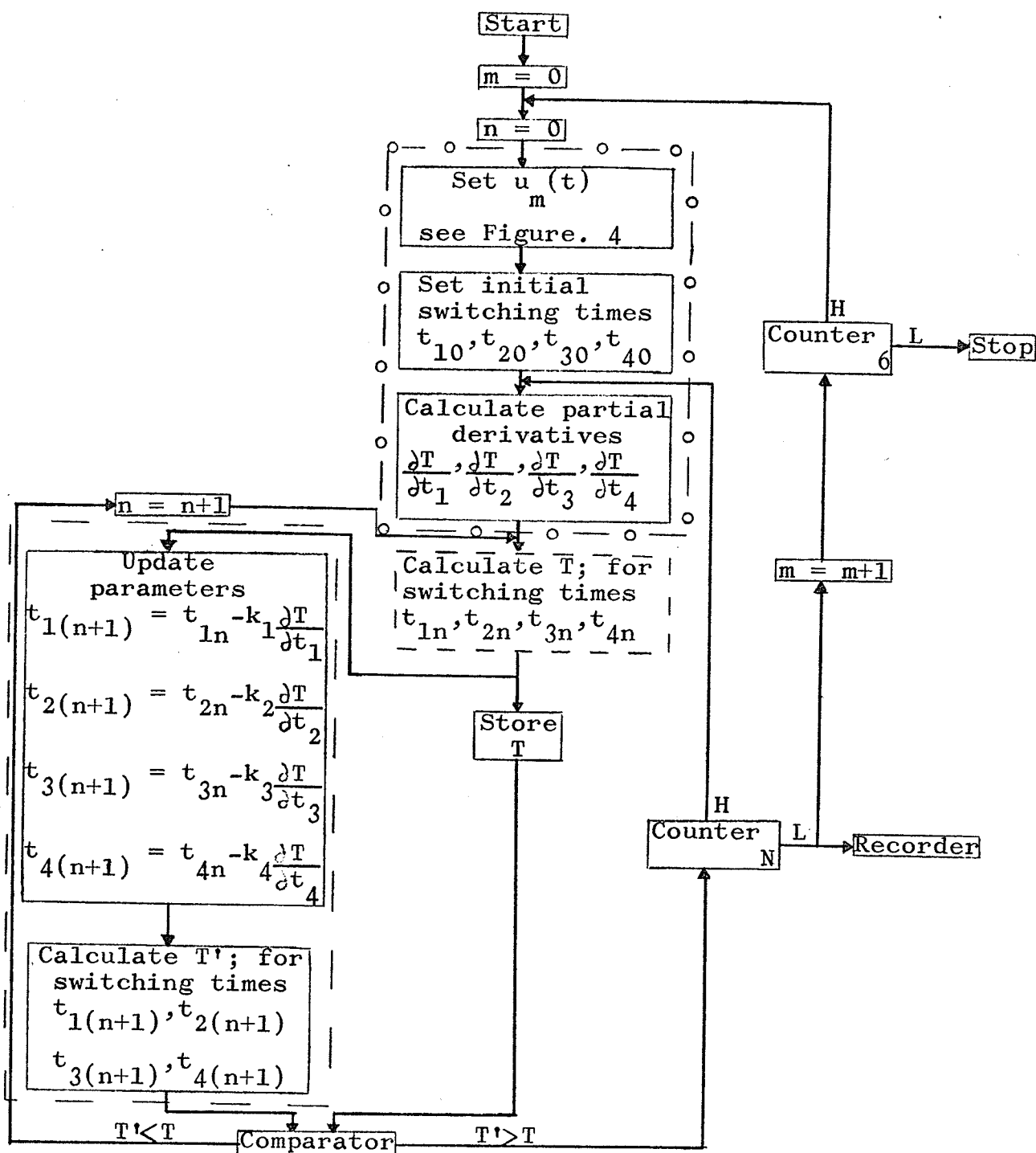


Figure 3. Block diagram of the iterative scheme

Exploration mode — o — o — o —
 Evaluation mode — — — — —
 Update mode — — — — —

$$\frac{\partial T}{\partial t_1} = \frac{T(t_1 + h/2, t_2, t_3, t_4) - T(t_1 - h/2, t_2, t_3, t_4)}{h}$$

$$\frac{\partial T}{\partial t_2} = \frac{T(t_1, t_2 + h/2, t_3, t_4) - T(t_1, t_2 - h/2, t_3, t_4)}{h}$$

$$\frac{\partial T}{\partial t_3} = \frac{T(t_1, t_2, t_3 + h/2, t_4) - T(t_1, t_2, t_3 - h/2, t_4)}{h}$$

$$\frac{\partial T}{\partial t_4} = \frac{T(t_1, t_2, t_3, t_4 + h/2) - T(t_1, t_2, t_3, t_4 - h/2)}{h}$$

As the switching instants approach their optimal values the partial derivatives approach zero (provided $h/2$ is sufficiently small) and the program will tend to remain or oscillate slightly around the optimal solution. A central difference method rather than a one-sided difference method was used, because of the fact that the program using a one-sided difference will have large oscillations around the optimal solution. As the measurement of the optimal switchings instants relies on the fact that the program will eventually settle down to the optimal solution, and remain there, a one-sided difference cannot be used.

Because there is a possibility of solutions at a local minimum the iterative scheme will, in turn, work out the time solution beginning with each of the $u(t)$ functions in Figure 4. By way of a counter a reasonable length of time,

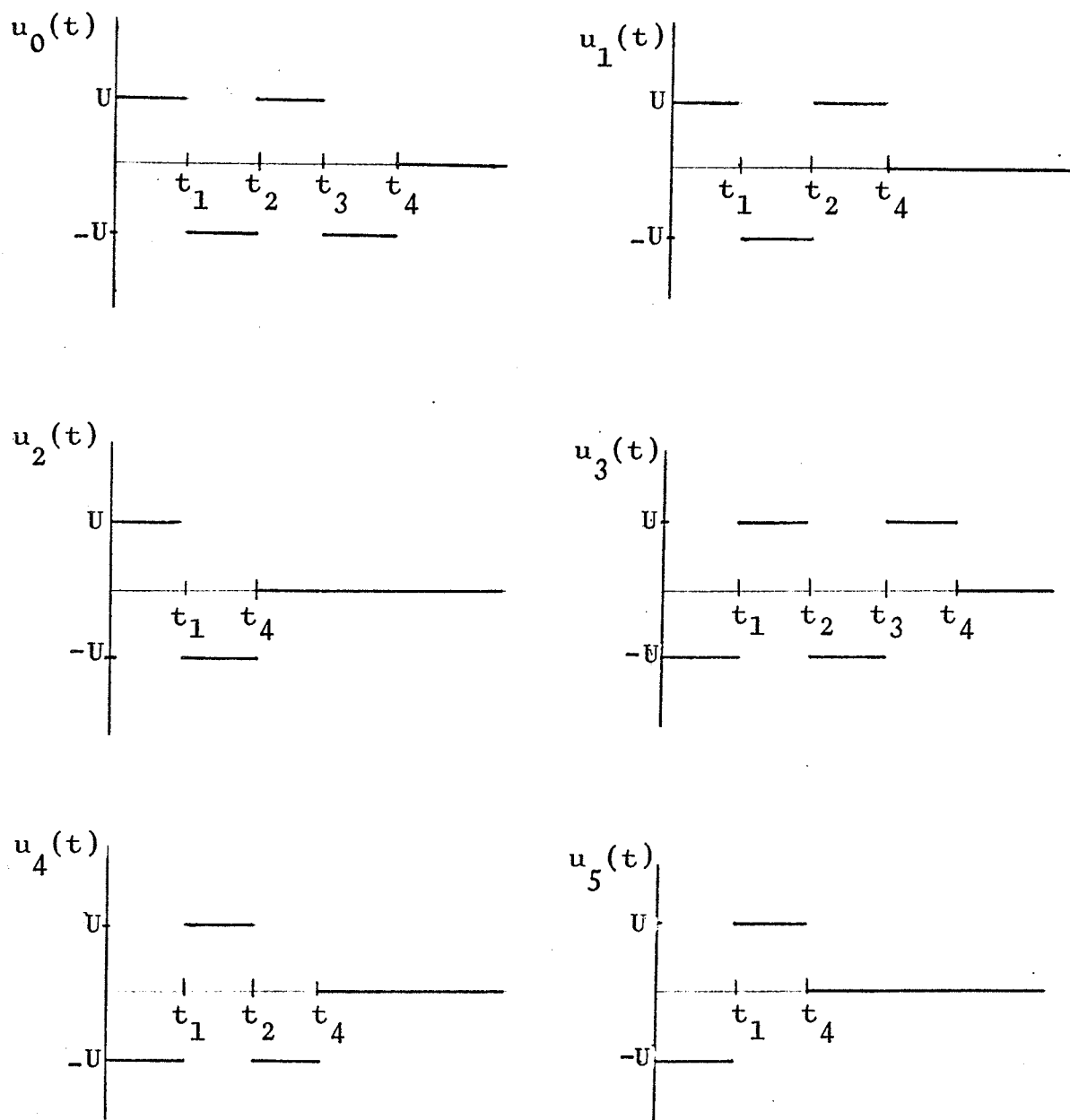


Figure 4. Control functions $u_m(t)$.

chosen at random, is allotted by the program for each time optimal solution to be found. As each solution is found the value of T and the optimal switching instants t_1 to t_4 will be stored by the recorder. A comparison of the six values of T will be made by the recorder and the switching instants t_1 to t_4 , yielding the smallest time T , will be stored.

CHAPTER IV

HYDRID COMPUTER PROGRAM

The complete analogue computer program is presented in Figure 5. The timing and the order of events is established by the logic part of the program, shown on the extreme left. Because the effect of the disturbance on the plant must be repeated many times in order to calculate partial derivatives, update parameters, etc., the computer is run in the repetitive operation mode. The IC (A) and OP (\bar{A})* periods are preset on the computer and fed into a flip flop, whose delay produces a sharp marking pulse, $E\bar{A}$, at the end of the operate period. By the use of a six bit ring shift register GPRO, the computer can be cycled through four exploration runs (Ex_1 to Ex_4), each consisting of two IC - OP periods, one evaluation run (Ev), consisting of a single IC - OP period, and one update run (U), consisting of a number of IC - OP periods. During the exploration runs (Ex_1 to Ex_4) the partial derivatives $\frac{\partial T}{\partial t_1}$, $\frac{\partial T}{\partial t_2}$, $\frac{\partial T}{\partial t_3}$, and $\frac{\partial T}{\partial t_4}$, respectively, are calculated. The pulse $E\bar{A}$ is used in shifting the computer mode through the four exploration runs. The values of the criterion function T, with the initial switching instants t_{1n} to t_{4n} , is calculated during the evaluation mode. Improvements in the criterion function

*The repetitive operation mode has two periods, the initial condition (IC) and operate (OP) periods, following one after the other, each of which has a separate adjustment on the computer for setting the length of time the computer will remain in each period.

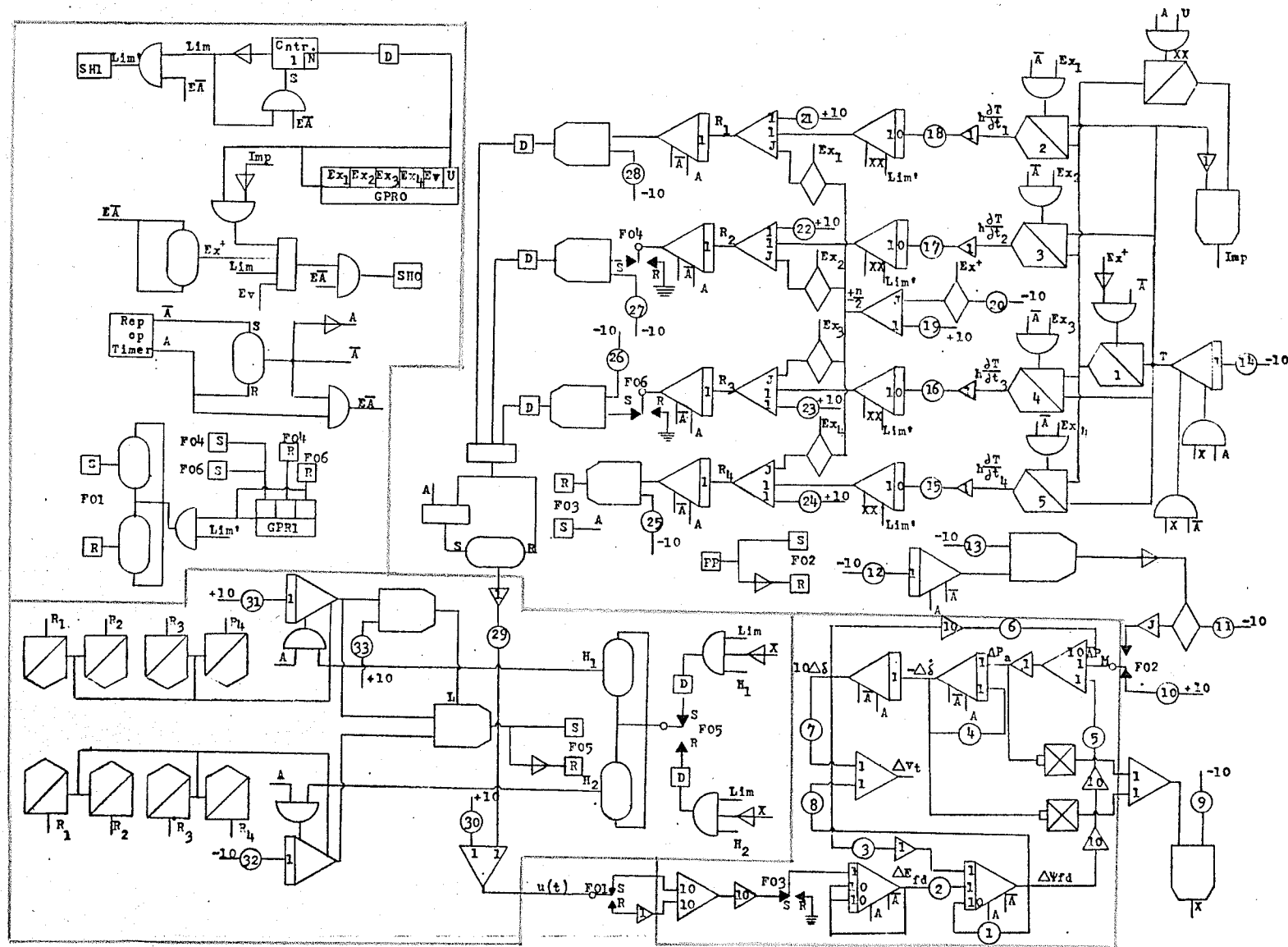


Figure 5. Analog Computer Program*

*Computer Symbols listed in Appendix

T are made during the update mode. As was mentioned earlier, as long as an improvement is made in T the computer will maintain the partial derivatives calculated and continue to update the parameters t_1 to t_4 . The signal Imp, which determines whether the program will remain in the update mode or shift to the Ex₁ mode, is high if an improvement in T has been made and low if there has been no improvement.

In the section explaining the modified gradient method, it was stated that each control function $u_m(t)$ in Figure 4 was allotted a definite time in which to reach the optimal solution. On the analogue computer this is accomplished by the use of counter 1, which counts the number of times the partial derivatives have been recalculated. Once the optimal solution has been found for a particular control $u_m(t)$, (see Figure 4), the next $u_m(t)$ function is substituted into the iterative scheme, by the use of a second ring shift register GPRI along with two flip flops.

To the right of the timing section is the network used to produce the control function $u_m(t)$. Initially function switches 01, 04 and 06 will be set, and the control input, $u_0(t)$ will be generated. As soon as counter 1 has counted up to N, the signal Lim goes high, resetting function switch 04 and generating the control function $u_1(t)$. In a similar manner the control functions $u_2(t)$ to $u_5(t)$ will be

generated in turn.

The plant, which is the Heffron and Phillips model of a synchronous generator, is shown in the lower right hand block of Figure 5. As a measure of the time it takes for oscillations in P_a , $\dot{\delta}$, and δ to damp out, the signal $\Delta P_a^2 + \Delta \dot{\delta}^2$ is formed and fed into a comparator; the output of which will be high as long as oscillations are still present, and will be low otherwise. Due to limitations of the computer components, the comparator will go low when $\Delta P_a^2 + \Delta \dot{\delta}^2$ is less than 0.01. Therefore the output of the comparator will indicate when oscillations in $\Delta \dot{\delta}$ and $\Delta \delta$ have been damped out below a constant level, rather than zero. The state variables $\Delta \Psi_{fd}$ and ΔE_{fd} have not been included here, because of the fact that oscillations in $\Delta \Psi_{fd}$ and ΔE_{fd} are relatively unimportant, compared with oscillations in $\Delta \dot{\delta}$, $\Delta \delta$ and ΔP_a . If $\Delta \Psi_{fd}^2$ and ΔE_{fd}^2 were included in $\Delta \dot{\delta}^2 + \Delta P_a^2$, the time T taken to damp out oscillations in $\Delta \dot{\delta}$, $\Delta \delta$ and ΔP_a^2 would undoubtedly be increased.

The generation of the criterion function T and the partial derivatives, the updating of the switching instants t_1 to t_4 , and the measurement of whether or not an improvement has been made in T, is accomplished by the network shown in the

top right hand corner of Figure 5. As the central difference method is being used to calculate partial derivatives, the parameters t_1 to t_4 have to be incremented by $\pm h/2$. The signals R_1 to R_4 will be incremented by $\pm n/2$, during the Ex_1 to Ex_4 modes, respectively. As the signals R_1 to R_4 control the switching instants t_1 to t_4 , an increment in R of $\pm n/2$ causes a corresponding increment of $\pm h/2$ in the switching instants t . The partial derivatives $\frac{\partial T}{\partial t_1}, \frac{\partial T}{\partial t_2}, \frac{\partial T}{\partial t_3}, \frac{\partial T}{\partial t_4}$

are produced during the Ex_1 to Ex_4 modes, respectively, and stored at the output of track and store units 2,3,4, and 5. During the IC period of the update mode, the values of R_1 to R_4 and thus t_1 to t_4 will be incremented by a value proportional to the negative of the partial derivatives

$\frac{\partial T}{\partial t_1}$ to $\frac{\partial T}{\partial t_4}$, respectively.

To clarify the above process, the calculation of

$\frac{\partial T}{\partial t_1}$ will be demonstrated. $\frac{\partial T}{\partial t_1}$ is calculated during the

Ex_1 mode. For the first IC - OP period the signal Ex^+ is low and the switching parameter t_1 will be incremented by $+h/2$ ($R_1 + n/2$). At the end of the OP period $-T(t_1 + h/2, t_2, t_3, t_4)$ will be stored by track and store unit 1. During the second IC - OP period Ex^+ is high and $h/2$ will be subtracted from t_1 . At the end of the OP period the quantity

$$T(t_1 + h/2, t_2, t_3, t_4) - T(t_1 - h/2, t_2, t_3, t_4) = h \frac{\partial T}{\partial t_1}$$

will be stored at the output of track and store unit 2.

In a similar manner $h \frac{\partial T}{\partial t_2}$, $h \frac{\partial T}{\partial t_3}$ and $h \frac{\partial T}{\partial t_4}$ will be stored at the

output of track and store units 3, 4, and 5 at the end of the Ex_2 , Ex_3 and Ex_4 modes, respectively.

The recorder is shown in the lower left hand block in Figure 5. This network will compare the criterion functions T calculated for each optimal control function $u_m(t)$ and will store the values of R and thus the optimal switching instants t_1 to t_4 which yield the smallest value of T . The mechanical torque disturbance inputs used are of the forms shown in Figure 6. When function switch 02 is set or reset the inputs of the form shown in Figure 6(a) or Figure 6(b), respectively, will be applied to the plant.

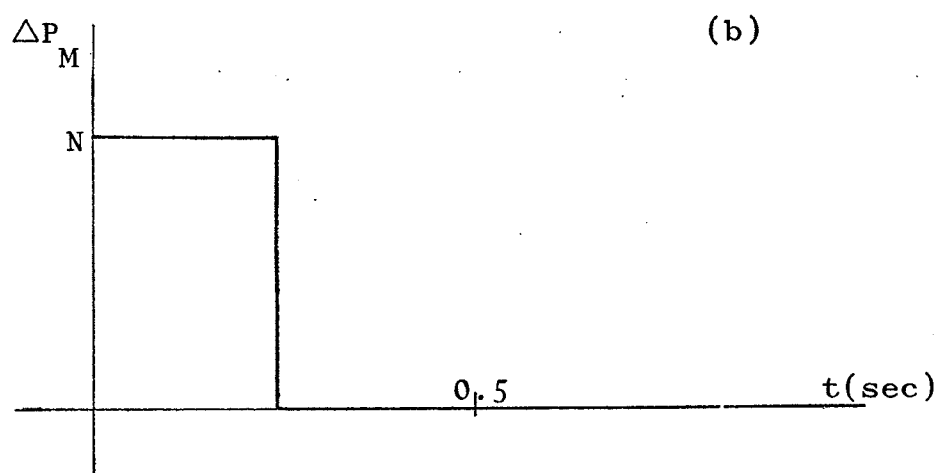
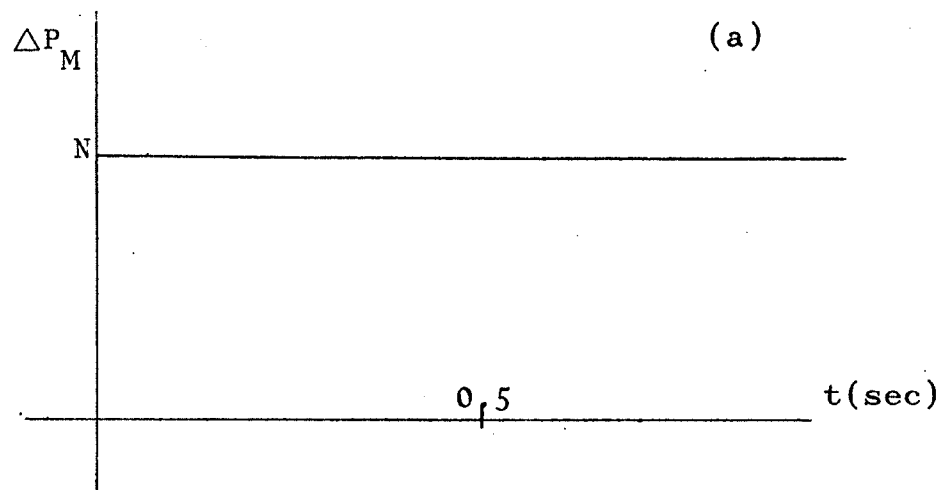


Figure 6. Mechanical torque input disturbances

CHAPTER V

EXPERIMENTAL RESULTS

The analogue computer program, shown in Figure 5, was simulated on an EAI 580 hybrid computer slaved with a TR - 20 analogue computer. As has been mentioned, the plant used is the Heffron and Phillips model of a synchronous generator connected to an infinite bus. The Heffron and Phillips constants, for various operating points, are presented in Table 1.²⁰ The time optimal control of a synchronous generator delivering rated power at unity power factor, with an external reactance of 0.0480 p.u., was determined and the results are shown in Figures 7 to 24. Two types of mechanical torque inputs have been applied to the plant, as shown in Figure 6. The results shown in Figures 7 to 20 were plotted using a mechanical torque input of the form shown in Figure 6(a), while the results shown in Figures 21 to 24 were plotted using a mechanical torque input of the form shown in Figure 6(b).

Figures 7 to 9 are phase plane plots of $\Delta\dot{\delta}$ vs $\Delta\delta$, $\Delta\psi_{fd}$ vs $\Delta\delta$ and $\Delta\psi_{fd}$ vs $\Delta\dot{\delta}$. The magnitude, U , of the control $u(t)$ was at first arbitrarily set at .058. The program was run and the optimal control $u^*(t)$ was found to be of the form

*
Table 1. Heffron and Phillips Constants
For Various Operating Points

p.f.	x_t (p.u.)	δ_o (Deg)	K_1	K_2	K_3	K_4	K_5	K_6
unity	.0480	20.3	1.63	.681	.623	.136	-.0244	.0863
0.8 Leading	.0480	14.4	1.36	.491	.623	.098	-.0210	.0886
0.8 Lagging	.0480	39.3	3.65	1.26	.623	.251	-.0446	.0735
unity	.200	31.5	1.30	.807	.680	.176	-.0892	.271
0.8 Leading	.200	18.0	1.06	.477	.680	.104	-.0650	.288
0.8 Lagging	.200	57.0	3.75	1.30	.680	.282	-.159	.215

$$T_e = 0.005 \text{ secs.}$$

$$K_e = 5.0$$

$$T'_{do} = .120 \text{ secs.}$$

$$M = .00165 \text{ p.u.}$$

$$D = .0114 \text{ p.u.}$$

* An extract from the M.Sc.EE thesis presented by G.W. Ryckman.²⁰

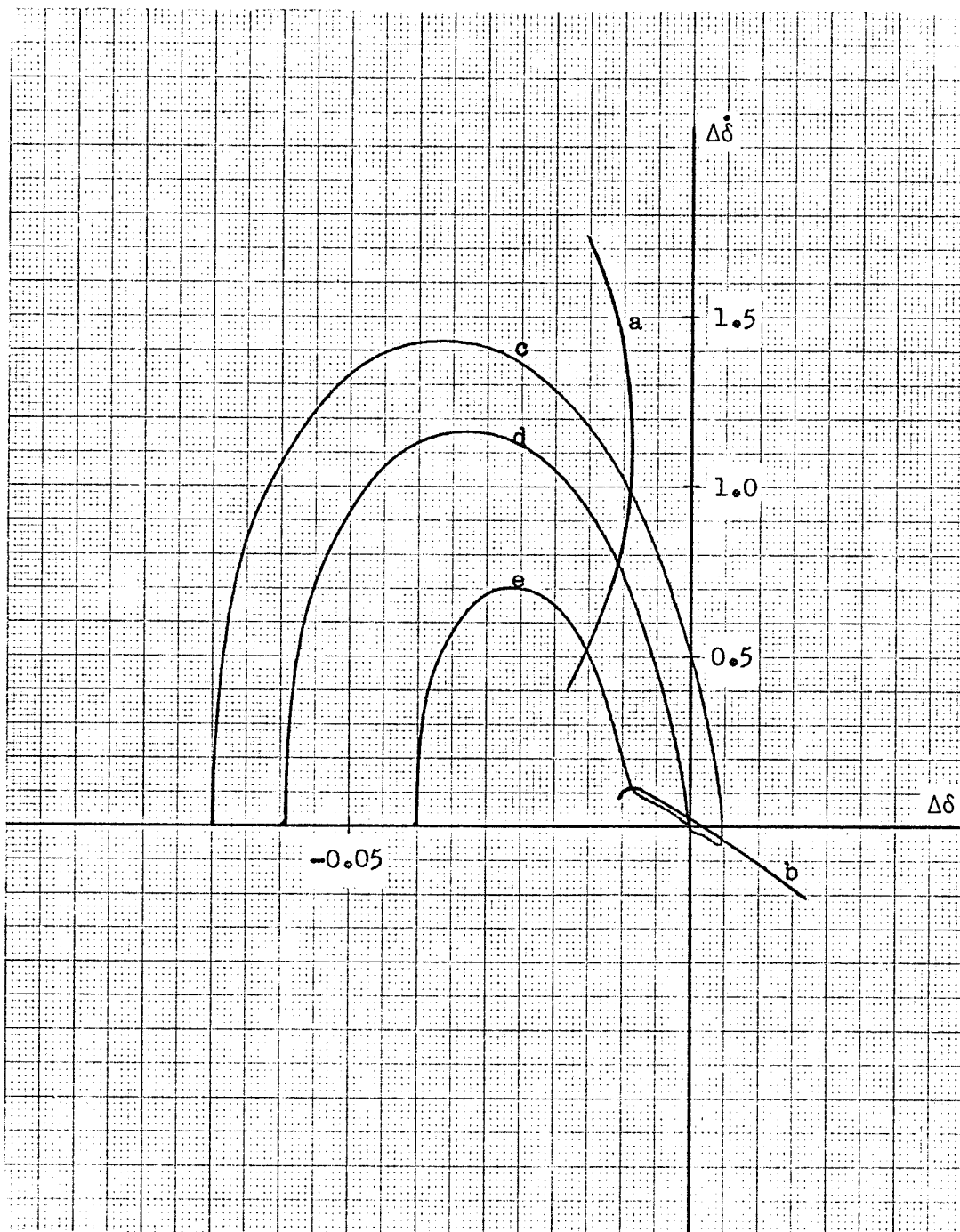


Figure 7. $\Delta\dot{\delta}$ versus $\Delta\delta$ showing optimal switching curves (a;b) for various torque input magnitudes ($c = .07$, $d = .096$, $e = .12$) (constant control magnitude)

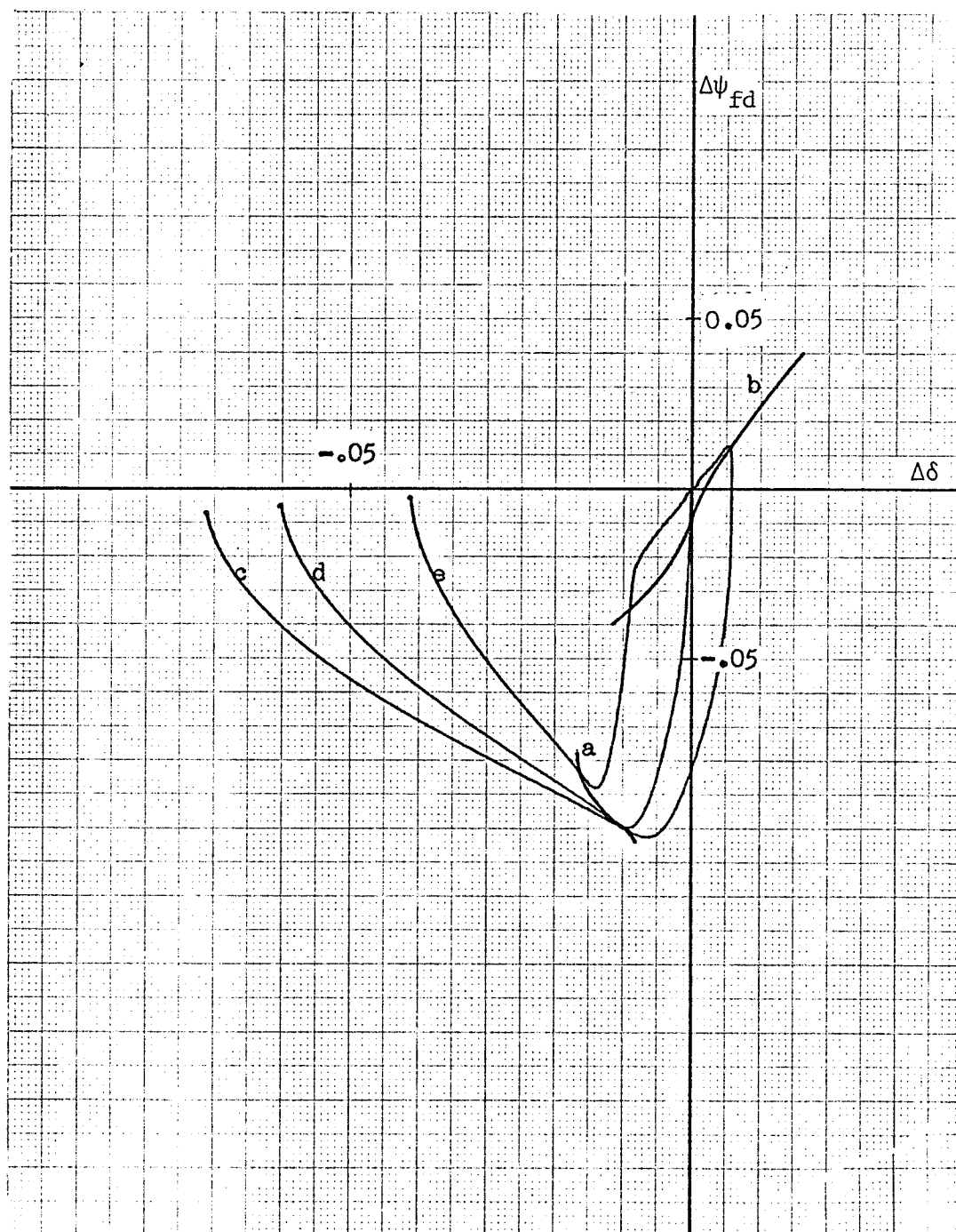


Figure 8. $\Delta\psi_{fd}$ versus $\Delta\delta$ showing optimal switching curves (a;b) for various torque input magnitudes ($c = .07$, $d = .096$, $e = .12$) (constant control magnitude)

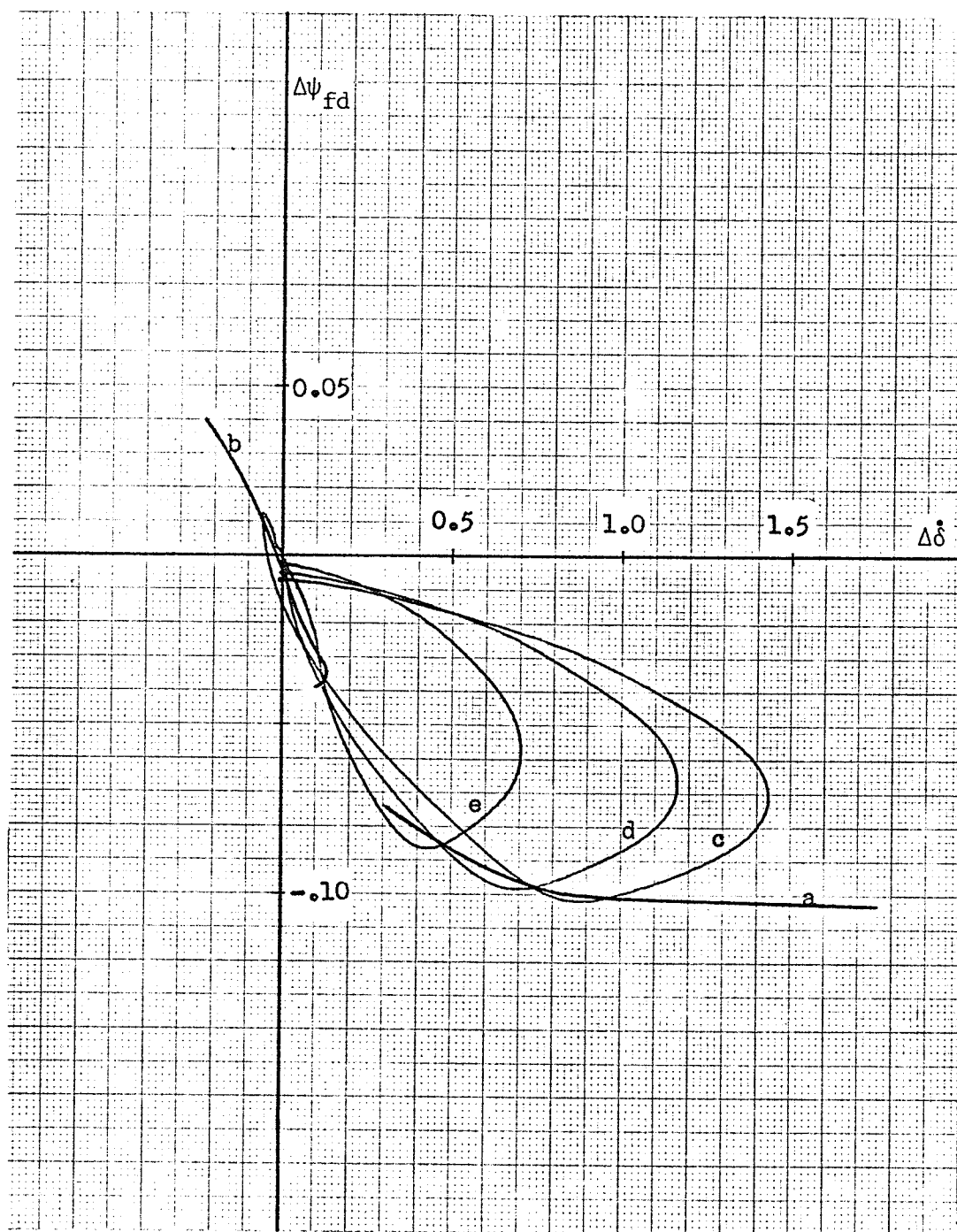
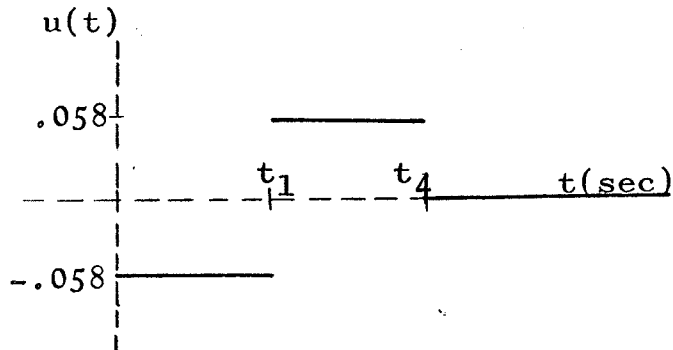


Figure 9. $\Delta\psi_{fd}$ versus $\Delta\dot{\delta}$ showing optimal switching curves (a;b) for various torque input magnitudes ($c = .07$, $d = .096$, $e = .12$) (constant control magnitude)



Curves a and b in Figures 7 to 9 show the magnitude of the state variables $\Delta \dot{\delta}$, $\Delta \delta$, and $\Delta \psi_{fd}$ at the optimal switching instants t_1 and t_4 , respectively, as the mechanical torque input (ΔP_M) was varied from .05 to .13 p.u. Typical time optimal trajectories, having mechanical torque input disturbances of .07, .096, and .12 are shown by curves c, d, and e, respectively. The switching instants t_1 and t_4 are indicated by the crossing of curves c, d, and e with curves a and b, respectively. Knowing the initial state and also the switching curves a and b, the time optimal control $u^*(t)$, for any initial condition point in state space, can be generated.

It was hoped that one set of switching instants, for $u(t)$, might be chosen that would serve fairly well for all magnitudes of disturbance due to a change in mechanical torque input. However, with disturbance input magnitudes

between the ranges of .05 to .13 the change in optimal switching instants was from .042 to .062 sec., for the first switch (t_1), and .059 to .112 sec. for the second switch (t_4). According to Pontryagin's principle, for a bounded control $u(t)$, the time optimal control $u^*(t)$ is generated by the use of the maximum possible magnitude U . However, after careful experimentation involving a variation in control magnitude U , under a constant disturbance magnitude N , (see Figure 10), it was concluded that the magnitude of control U , yielding a time optimal solution, directly affected the damping out time T .*

Figure 10 presents the time optimal trajectories of $\Delta\dot{\delta}$ and $\Delta\delta$ versus time for a disturbance input magnitude of 0.1 and control input magnitudes of 0.07, and 0.06 and 0.042; shown in curves a,b and c, respectively. While curves a and c represent the time optimal solution for the particular control magnitudes 0.07 and 0.042, it is evident that curve b, with a control magnitude of 0.06, definitely yields the shortest time T . Furthermore, it was found that this was the general case for all magnitudes of disturbance input. Figure 11 is a plot of mechanical torque input versus control input magnitude U . For a particular disturbance input the corresponding control input, indicated in Figure 11, has to be used in order for the iterative scheme to produce

*See end of this chapter.

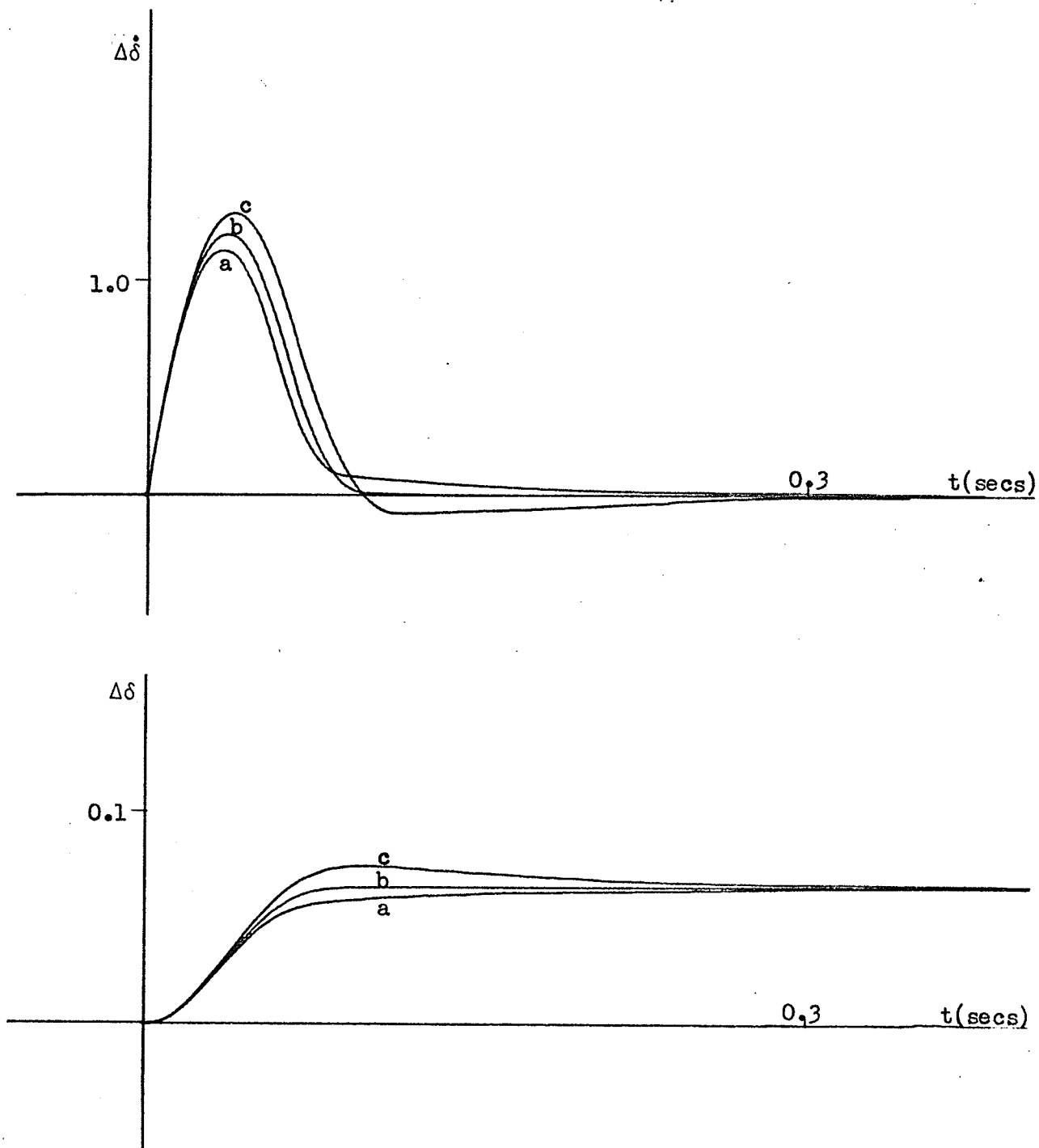


Figure 10. Dynamic stability of $\Delta\dot{\delta}$ and $\Delta\delta$ with time optimal control.
 Constant disturbance input magnitude (0.1)
 Variable control magnitude ($a = 0.07$, $b = 0.06$, $c = 0.042$)

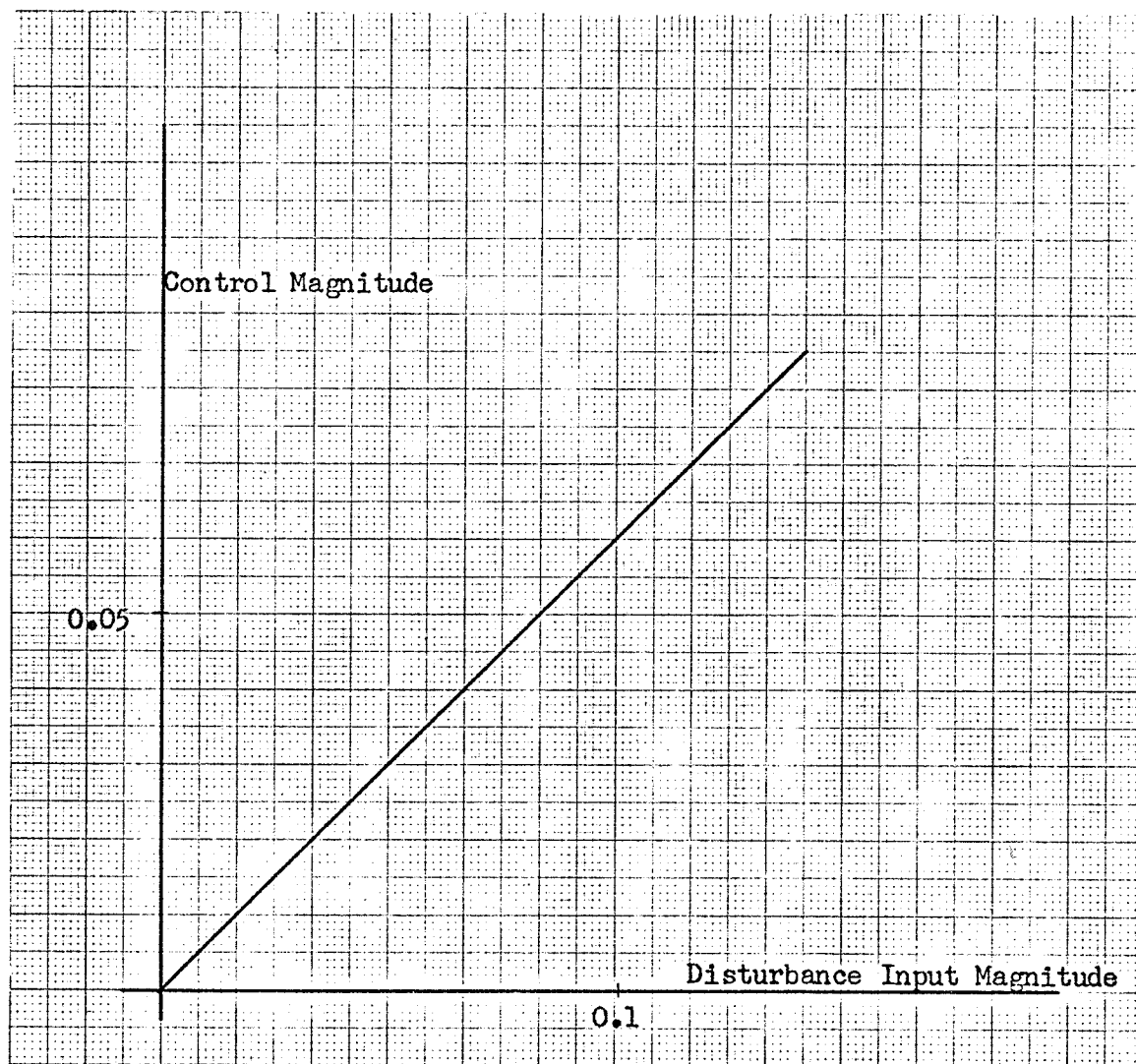
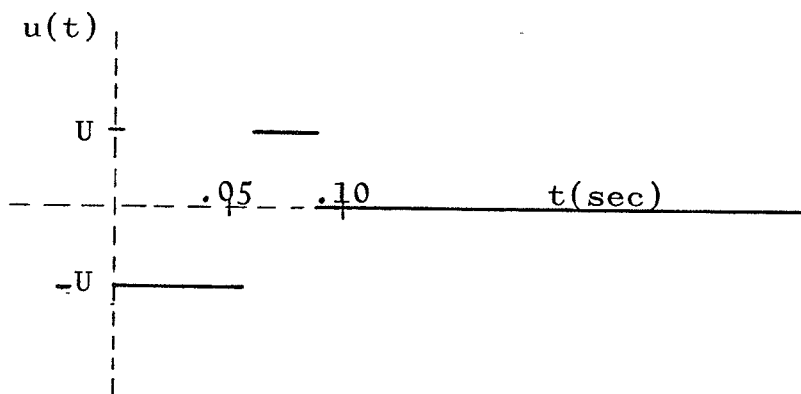


Figure 11. Relationship between control and input magnitude yielding time optimal control

an optimal solution $u^*(t)$, yielding the shortest time T .

The data in Figures 12 to 19 were taken utilizing Figure 11. It was found that the optimal control, for various magnitudes of mechanical torque inputs was of the form



with the magnitude U , variable, (according to Figure 11) and the switching instants t_1 and t_4 constant at .058 and .0944 sec., respectively. Figures 12 and 13 are plots of $\dot{\Delta\delta}$, $\Delta\delta$, $\Delta\psi_{fd}$ and Δv_t vs time, for input magnitudes of 0.033, 0.066, 0.099 and 0.132. Superimposed on these curves are two lines indicating the place where the two switching instants t_1 and t_4 occur. Figures 14, 15 and 16 are the optimal phase plane plots of $\dot{\Delta\delta}$ vs $\Delta\delta$, $\Delta\psi_{fd}$ vs $\Delta\delta$ and $\Delta\psi_{fd}$ vs $\dot{\Delta\delta}$, for input magnitudes of .033, .066, .099 and .132. Superimposed on these curves is a line indicating the point where the first switching occurs. For clarity, the second switching line has been omitted.

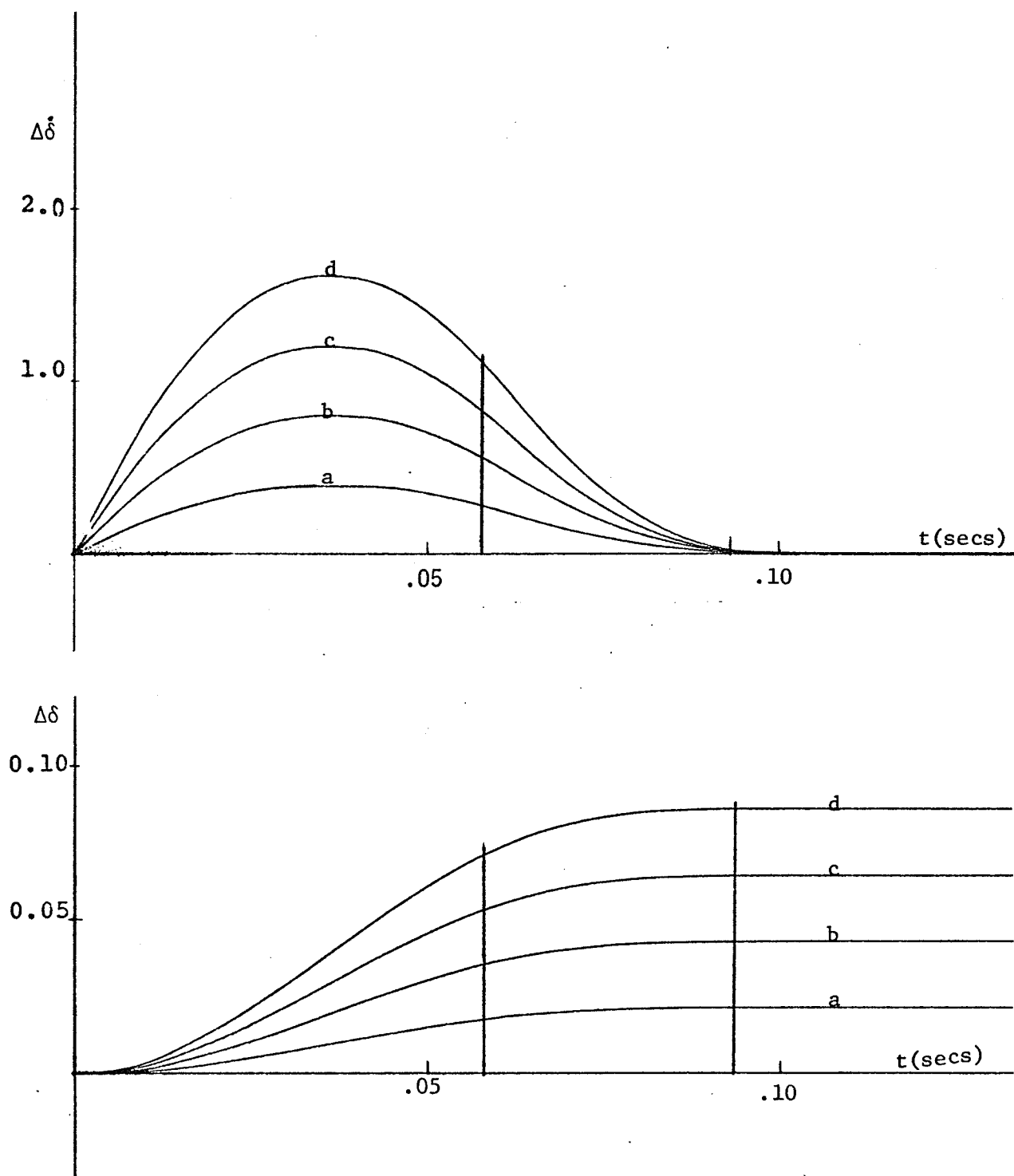


Figure 12. Time optimal solution of $\Delta\dot{\delta}$ and $\Delta\delta$ input magnitude a)0.033 b)0.066 c)0.099 d)0.132

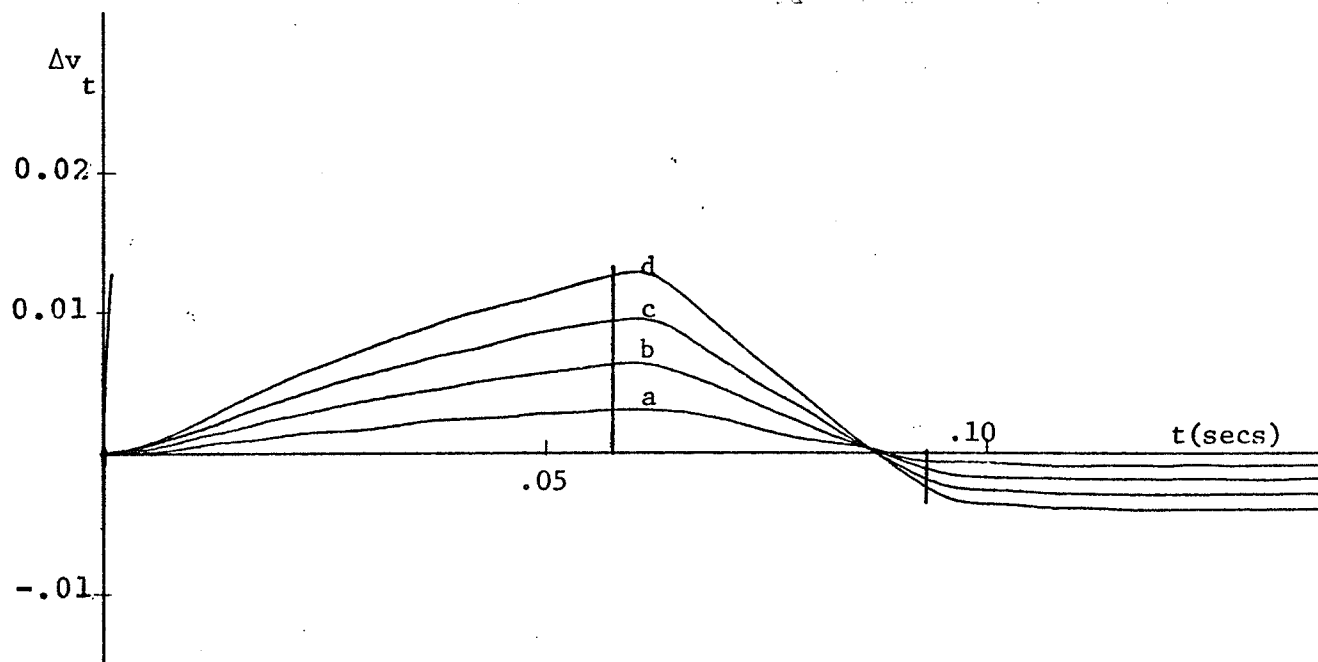
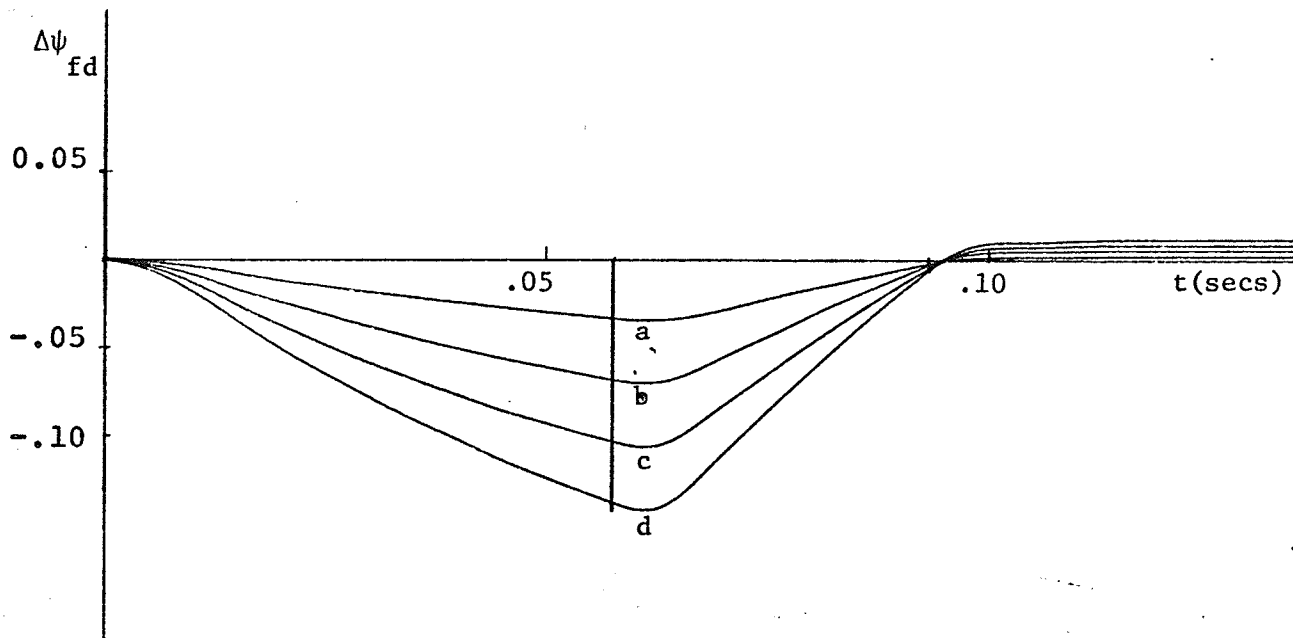


Figure 13. Time optimal solution of $\Delta\psi_{fd}$ and Δv_t
input magnitude a) 0.033 b) 0.066 c) 0.099
d) 0.132

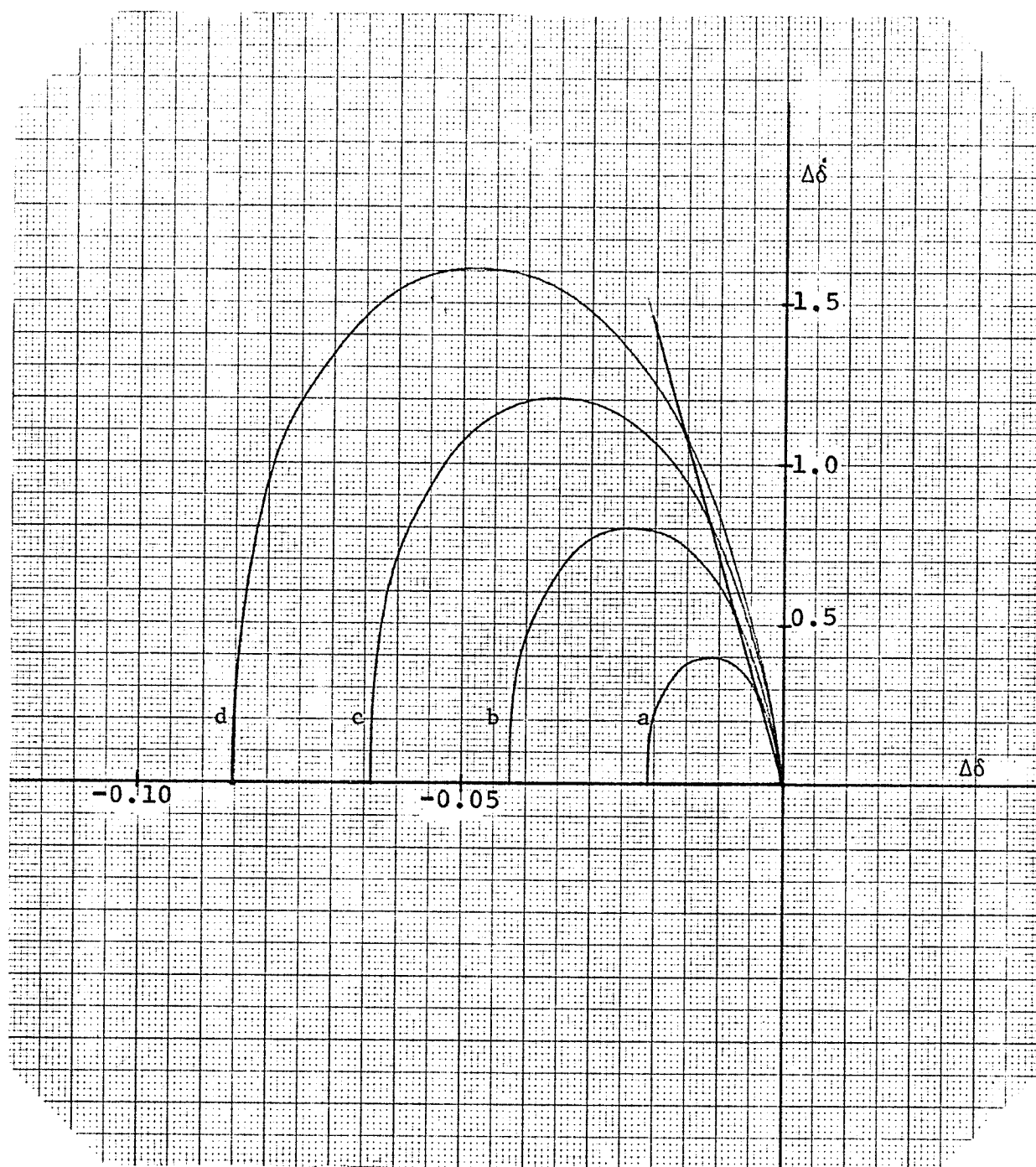


Figure 14. Time optimal trajectories in the $\Delta\dot{\delta}$ versus $\Delta\delta$ plane, input magnitudes a)0.033 b)0.066 c)0.099 d)0.132, control magnitudes a)0.02 b)0.04 c)0.06 d)0.08

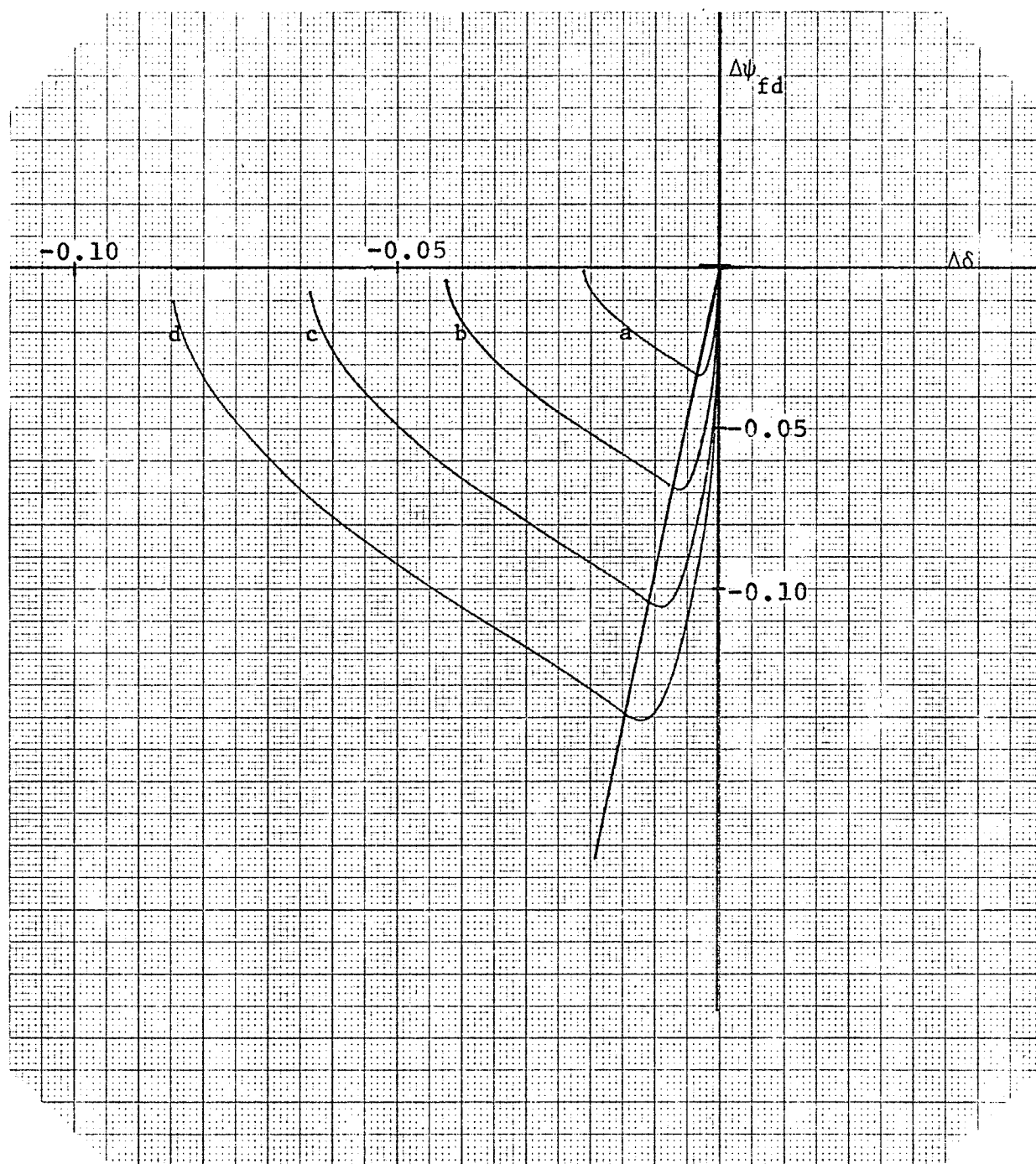


Figure 15. Time optimal trajectories in the $\Delta\psi_{fd}$ versus $\Delta\delta$ plane, input magnitudes a)0.033 b)0.066 c)0.099 d)0.132, control magnitudes a)0.02 b)0.04 c)0.06 d)0.08

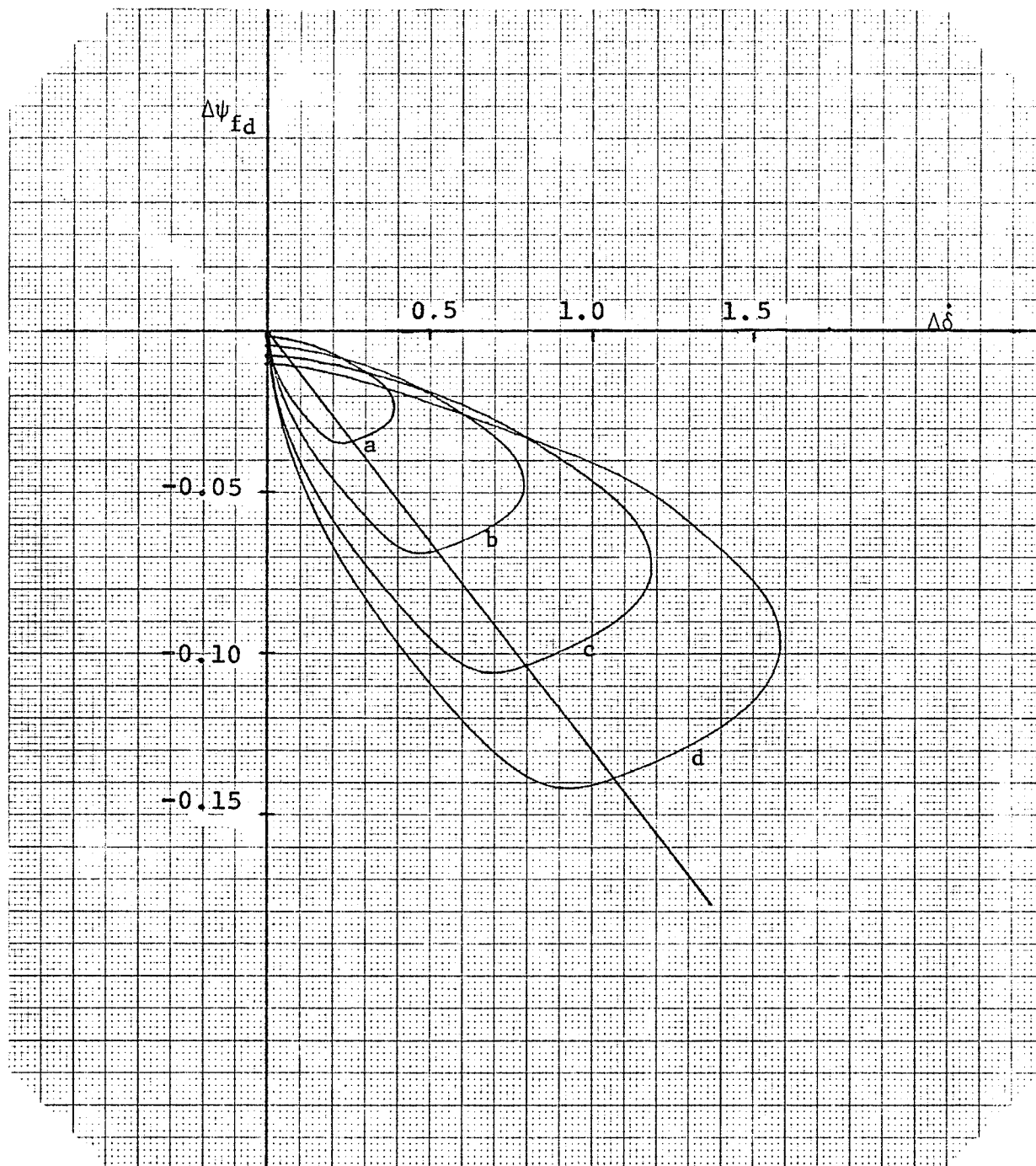


Figure 16. Time optimal trajectories in the $\Delta \psi_{fd}$ versus $\Delta \dot{\delta}$ plane, input magnitudes a)0.033 b)0.066 c)0.099 d)0.132, control magnitudes a)0.02 b)0.04 c)0.06 d)0.08

Figure 17 shows particular stages of the iterative process as seen from the $\Delta\dot{\delta}$ vs $\Delta\delta$ phase plane. Plot 1 shows the trajectory followed with no control present. Plot 2 shows the trajectory followed with any control, chosen at random. Plot 3 to 8 show various stages of the trajectory of the iterative program taken during the update mode. It is to be noted that in going from plot 6 to 7 the computer has passed the optimal solution. All modes were then repeated and the time optimal trajectory was found as shown in Figure 8. The operation time of the iterative process was variable taking anywhere from a few minutes up to ten to fifteen minutes. The main reason for this is the initial choice of the switching instants t_1 to t_4 . The closer the choice of initial switching instants to their optimal values, the shorter the operation time. The operation time was also affected to a large extent by the choice of parameters for the iterative scheme. The parameters of the iterative scheme are the values of $h/2$ and the k values k_1 to k_4 , which determine the amount by which the switching instants t_1 to t_4 , respectively, are updated during the IC period of the update mode. It was found that while these parameters could be optimally chosen to yield the fastest operation time for a certain input magnitude; as the disturbance input magnitude was varied, the parameters had to be changed in order to maintain the same

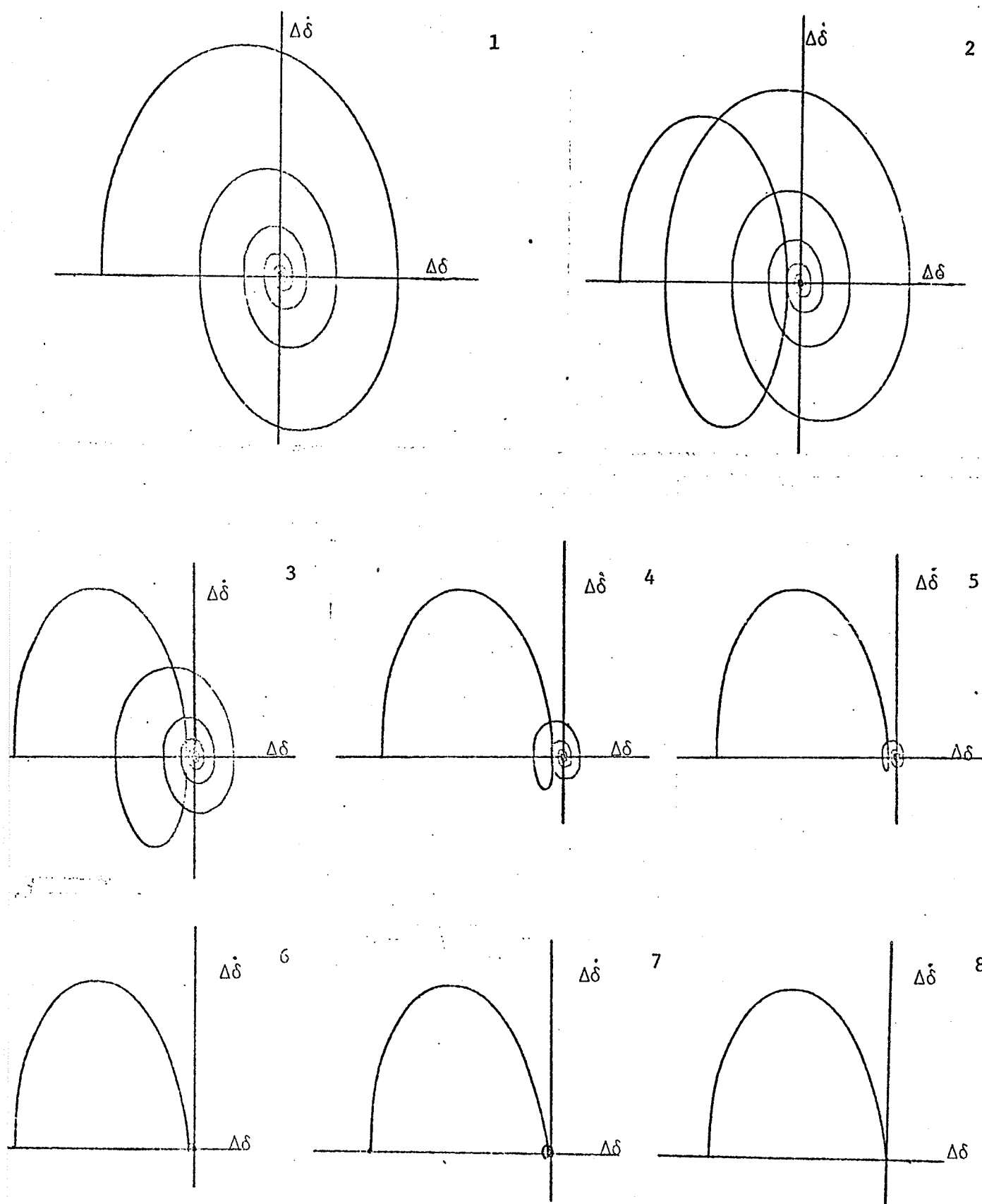


Figure 17. Steps in iterative scheme

operation time. As a result a set of parameters was used which gave a reasonable operation time for all disturbance input magnitudes.

Figures 18 and 19 show plots of $\Delta\delta$, $\Delta\dot{\delta}$, ΔP_a , $\Delta\psi_{fd}$ vs time without any control and with the optimal control present. It can be seen that the oscillations in $\Delta\dot{\delta}$, $\Delta\delta$ and $\Delta\psi_{fd}$ with optimal control present, have definitely been damped out more quickly. It is to be noted that there is a large jump in terminal voltage initially and also that the change in terminal voltage does not return to zero. Both of these disadvantages to the system pose no problem due to the relatively small magnitude of change. The jump in terminal voltage is only .007 and the change in terminal voltage is only .003. With large magnitudes of disturbance the change in terminal voltage can reach .010 to .015 p.u. This change in terminal voltage, however, will not bother the system for a short time and can eventually be dissipated by disconnecting the bang bang control and feeding the terminal voltage into the exciter through a suitable R-C network which will bring it back to zero without causing significant oscillations in $\Delta\dot{\delta}$ and $\Delta\delta$.

For comparison purposes, a page from Gordon W. Ryckman's M.Sc. thesis has been included (See Figure 20). As with the curves in Figures 18 and 19 the disturbance

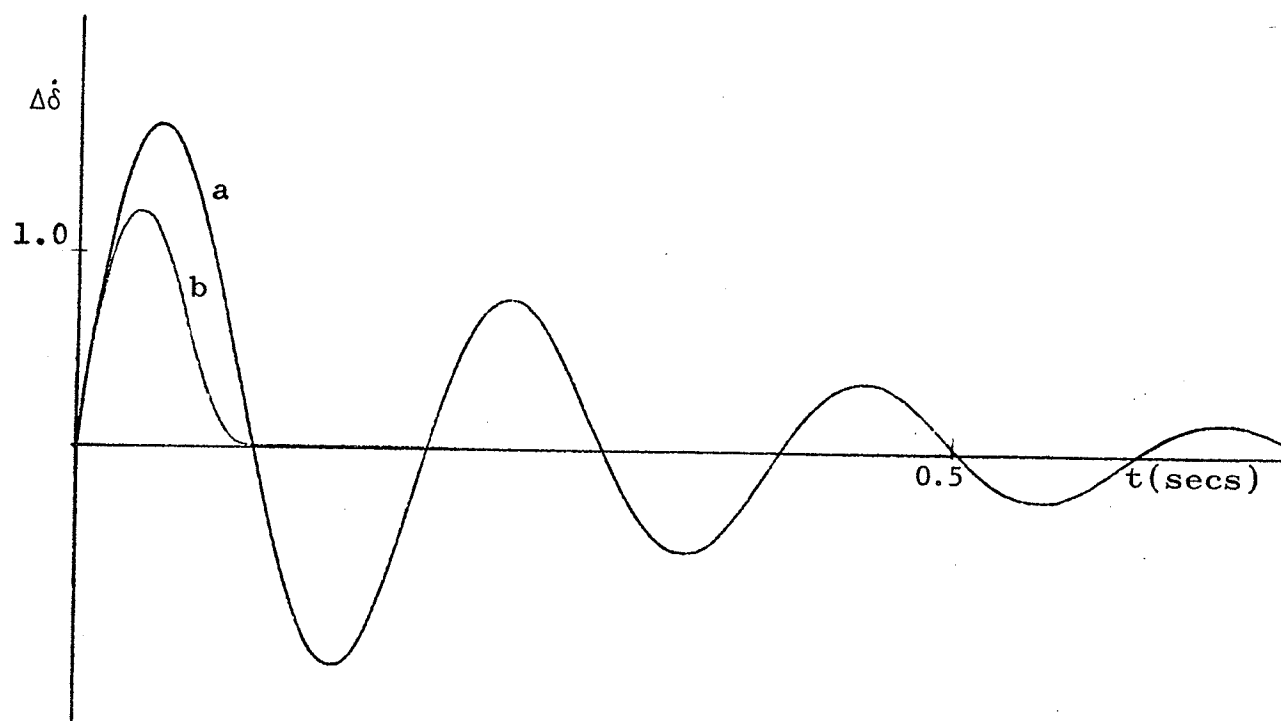
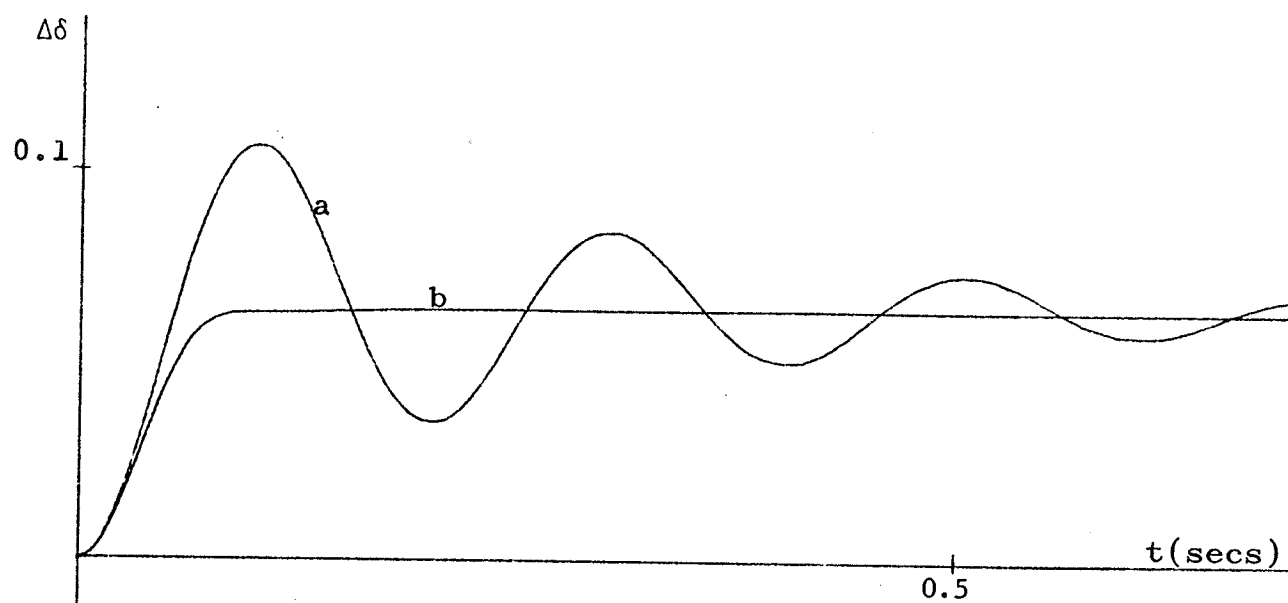


Figure 18. Dynamic stability of $\Delta\dot{\delta}$ and $\Delta\delta$, with no control (a) and with optimal control (b)

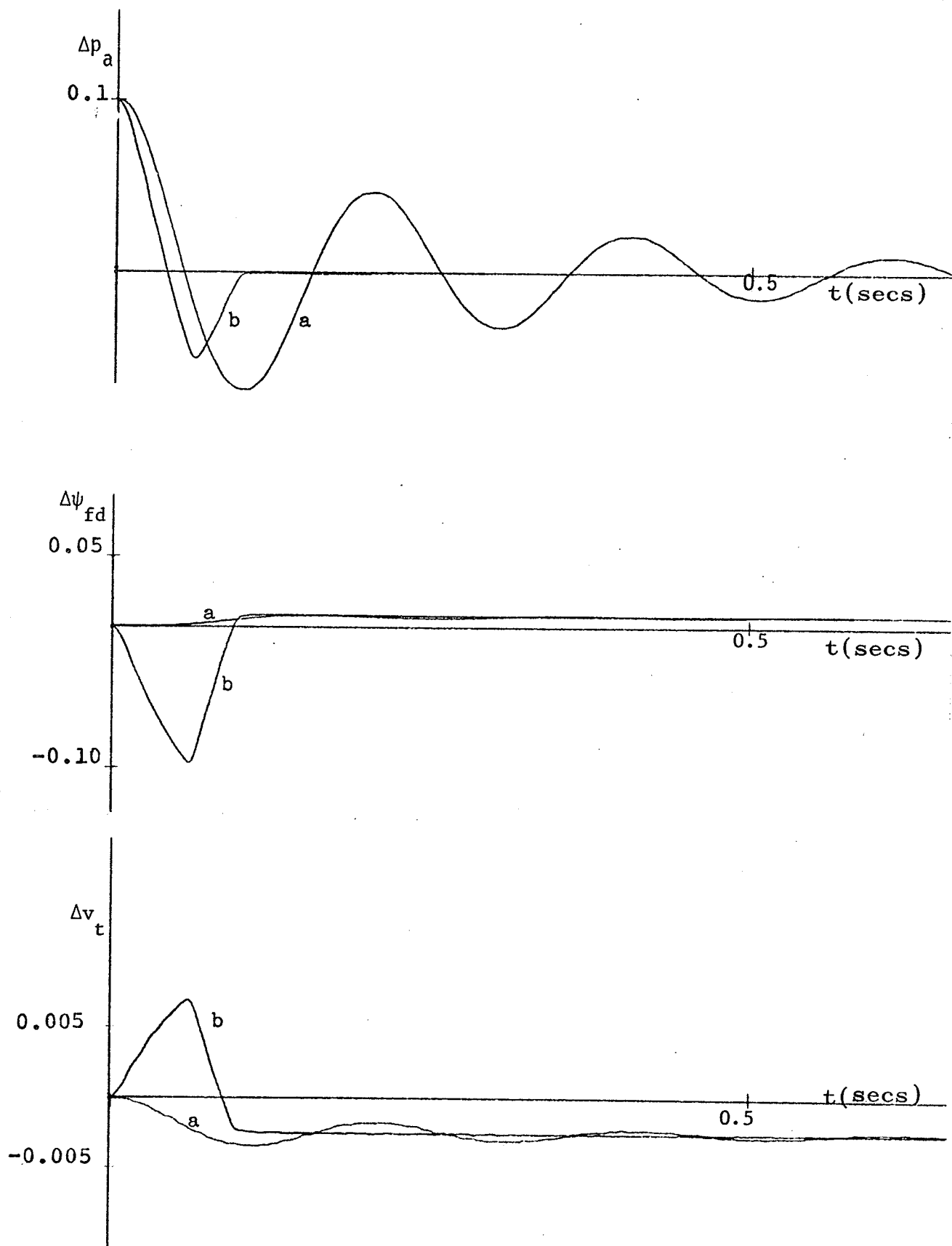


Figure 19. Dynamic stability of ΔP_a , $\Delta \psi_{fd}$ and Δv_t , with no control (a) and with optimal control (b)

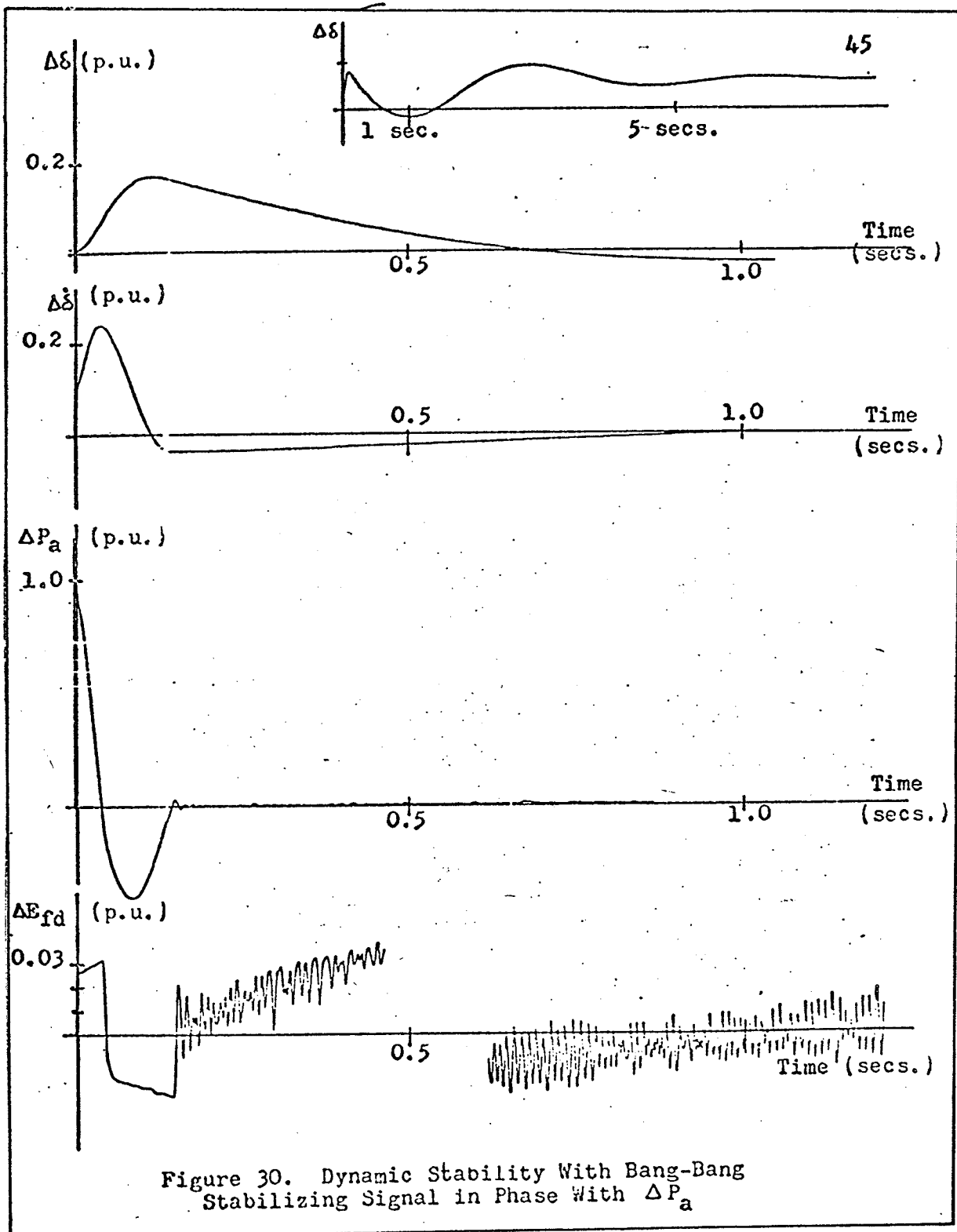


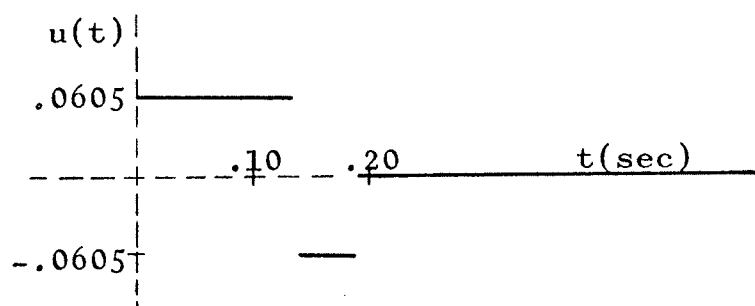
Figure 30. Dynamic Stability With Bang-Bang Stabilizing Signal in Phase With ΔP_a

Figure 20. Experimental results from an M.Sc.EE thesis presented by

G.W. Ryckman²⁴

magnitude was made equal to a change of 0.1 p.u. in the mechanical torque input. On comparing the time taken to damp out oscillations in $\Delta\dot{\delta}$, $\Delta\delta$, and ΔP_a one can see that by the use of optimal control theory oscillations in $\Delta\dot{\delta}$ have been damped out approximately 10 times faster, oscillations in $\Delta\delta$ approximately 100 times faster and oscillations in ΔP_a approximately twice as fast. The time taken to damp out oscillations completely was used here, for comparison purposes. If the computer limit, $(\Delta P_a^2 + \Delta\dot{\delta}^2 < 0.01)$ had been considered, the improvement in $\Delta\dot{\delta}$ would have been approximately twice as great using the iterative scheme as compared with G. W. Ryckman's solution.

Figures 21 to 24 present the results for input disturbance magnitudes of the form shown in Figure 6(b). For this disturbance two solutions were found which provided a great improvement over the uncompensated system. The $\Delta\dot{\delta}$ vs $\Delta\delta$ phase plane plot of the time optimal solution is shown in Figure 21 (b), with the corresponding uncompensated response shown in Figure 21 (a). The optimal control input is of the form



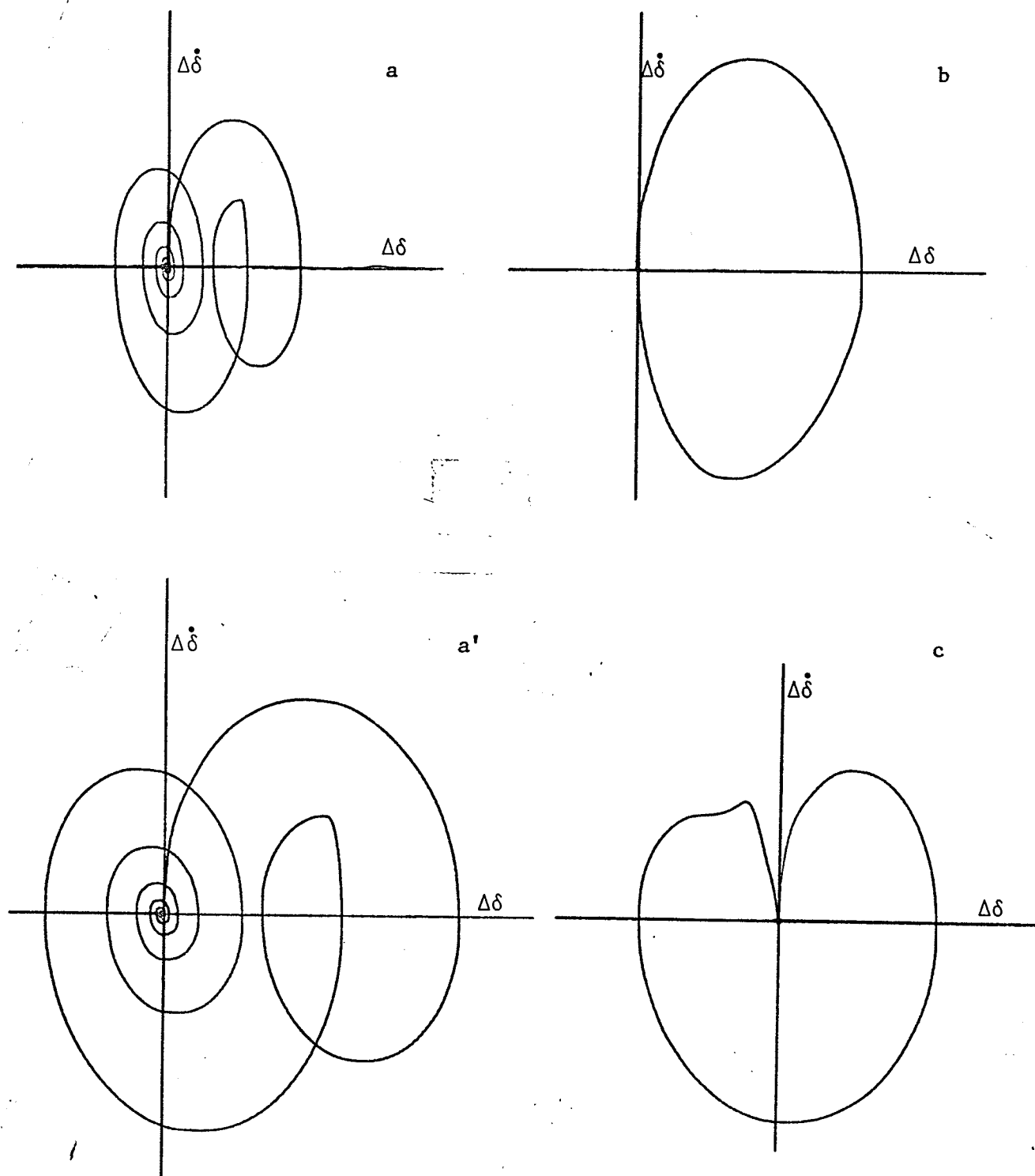


Figure 21. $\Delta\dot{\delta}$ versus $\Delta\delta$ phase plane plot for

- a) Uncompensated case b) Time - optimal case
 a') Uncompensated case c) Sub - optimal case

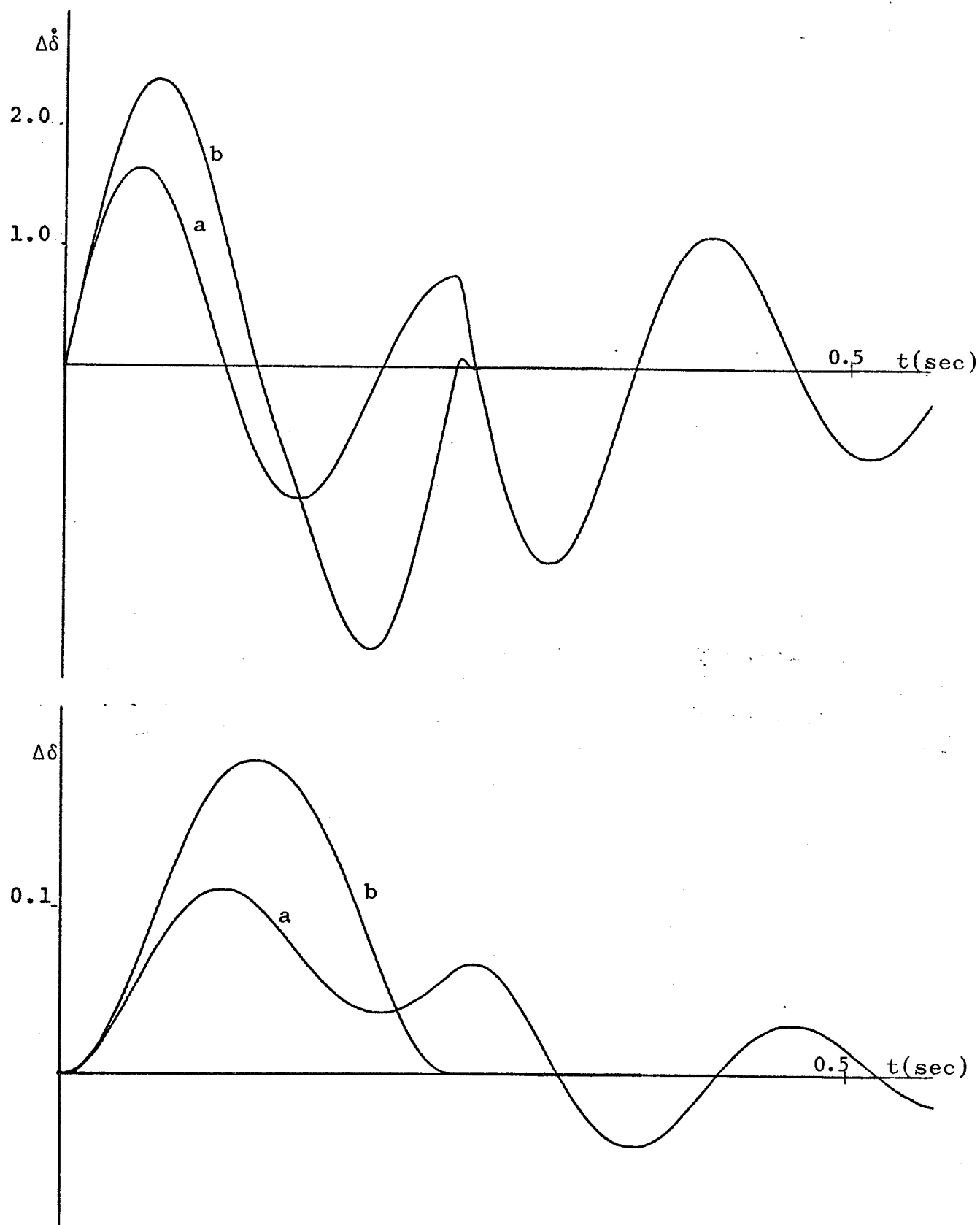


Figure 22. Dynamic stability of $\Delta\dot{\delta}$ and $\Delta\delta$ with no control (a) and with time optimal control (b)

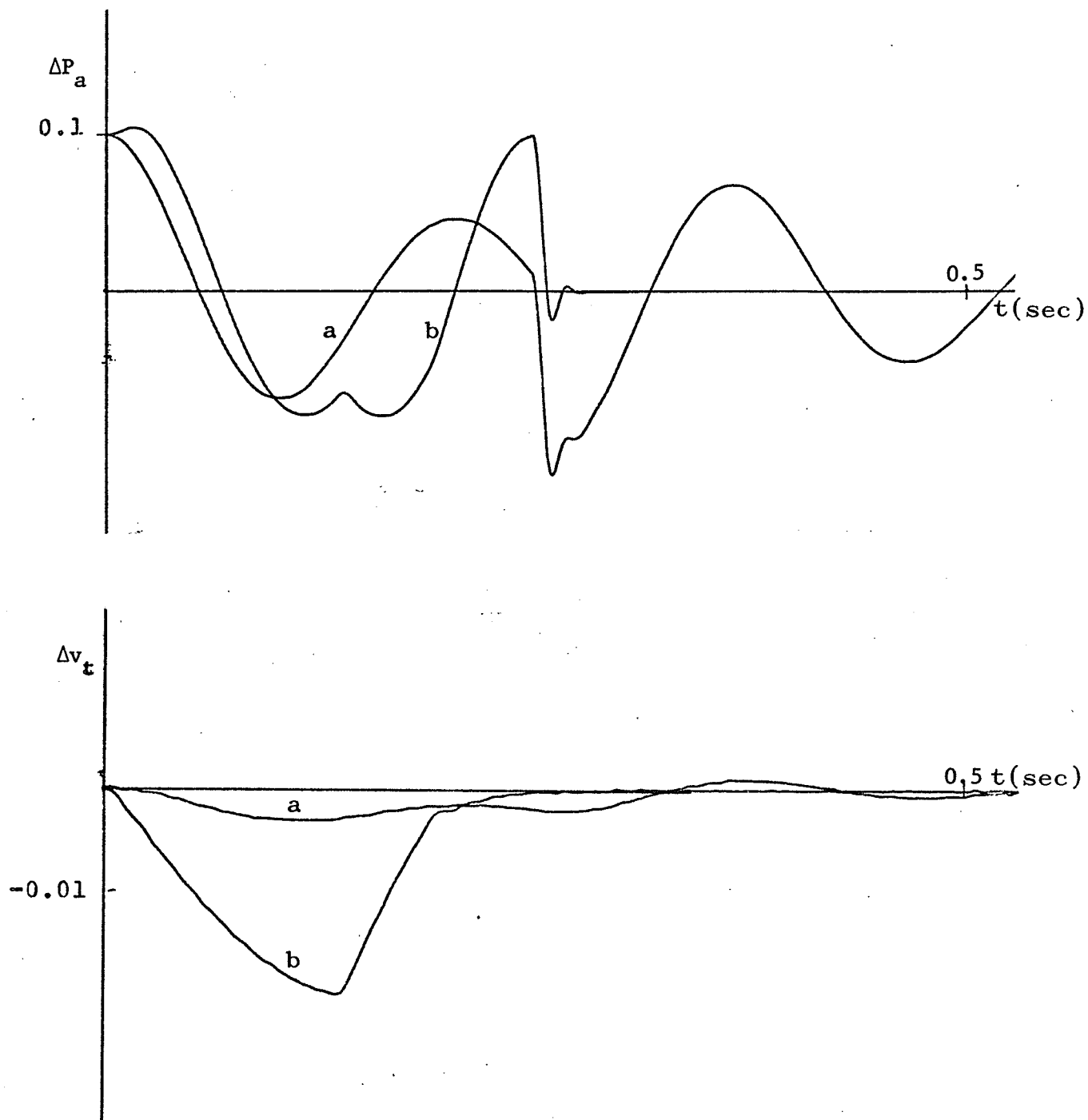


Figure 23. Dynamic stability of ΔP_a and Δv_t with no control (a) and with time optimal control (b)

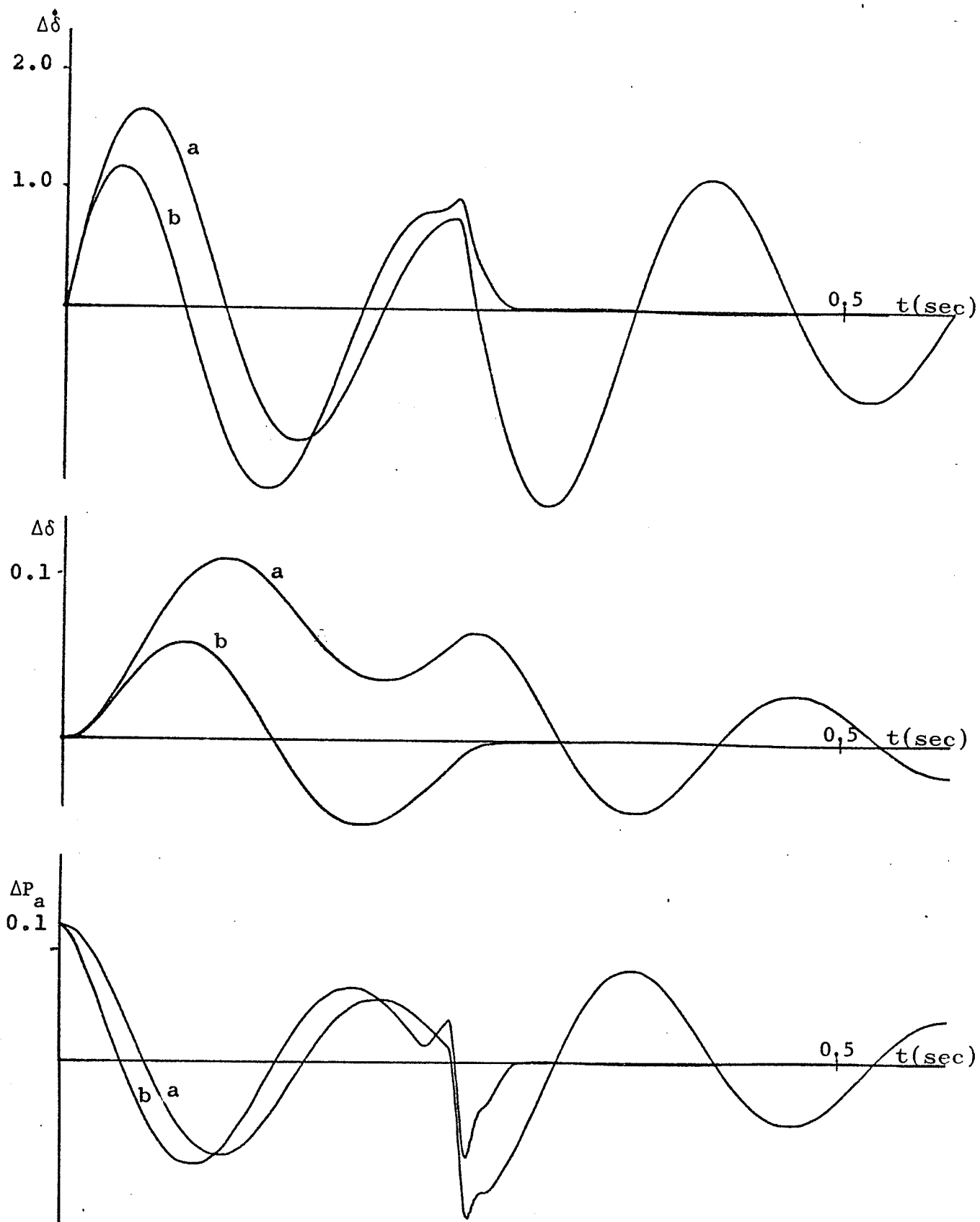
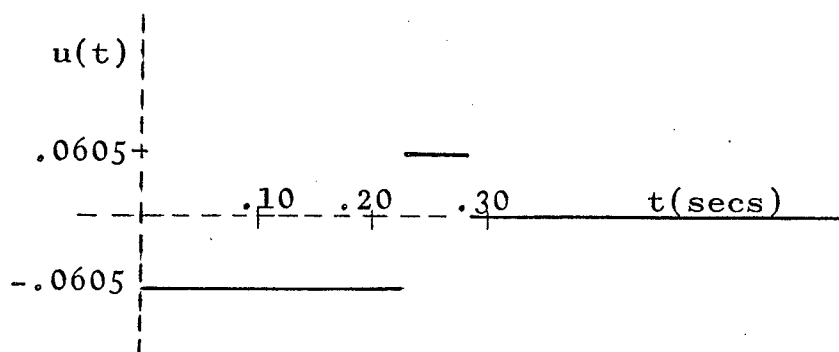


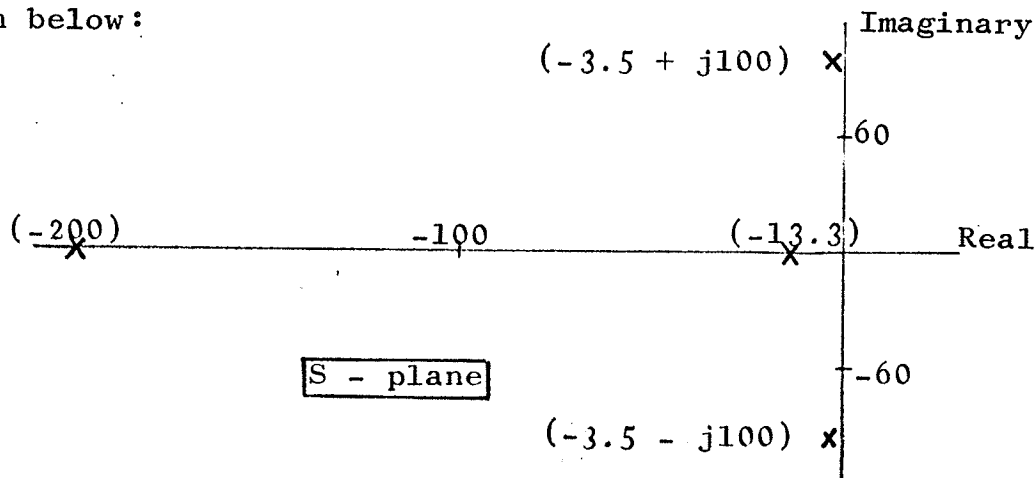
Figure 24. Dynamic stability of $\Delta \dot{\delta}$, $\Delta \delta$ and ΔP_a with no control (a) and with sub - optimal^a control (b)

where the input disturbance was 0.1 p.u. and the switching instants occurred at .134 and .190 secs. The $\Delta\dot{\delta}$ versus $\Delta\delta$ phase plane plot of the sub - optimal solution is shown in Figure 21 (c), with the corresponding uncompensated response shown in Figure 21 (a'). The control input is of the form



where the input disturbance was 0.1 p.u. and the switching instants occurred at .233 and .282 secs. Figures 22 and 23 present the dynamic stability of $\Delta\dot{\delta}$, $\Delta\delta$, ΔP_a and Δv_t with no control and with optimal control present. As can be seen there is once again a tremendous improvement in the time taken to damp out oscillations, with a damping out time of approximately .255 secs. For an input disturbance magnitude of the form shown in Figure 6(b), a very good sub - optimal case was found. The $\Delta\dot{\delta}$, $\Delta\delta$ and ΔP_a versus time plots, for this sub - optimal case, are shown in Figure 24. For this case the time taken to damp out oscillations is approximately .295 secs.

As has been stated, Pontryagin's principle seems to be in disagreement with the experimental results. A possible reason for this discrepancy lies in the fact that the signal $\Delta P_a^2 + \Delta \dot{\delta}^2$ has a limit on it. This limit, which has been set at $\Delta P_a^2 + \Delta \dot{\delta}^2 < 0.01$, changes the target set. The actual shape of the target set in four dimensional state space is very hard to predict, due to the fact that P_a^2 , which is not a state variable, is used in determining the target set. With a target set being something other than the origin, it is postulated that the computer program finds a solution which brings the trajectory to the new target set in the smallest possible time but not necessarily to the origin in the smallest possible time. With another trajectory being postulated as possible, the question arises as to why the program does not at any time happen to follow this trajectory. There are two possible explanations. As was mentioned earlier the plant has two real and two imaginary eigenvalues, shown below:



The complex conjugate roots are very close to the imaginary axis compared with the real roots, and hence dominate the program initially. For this reason the program does not anticipate another optimal solution. The resulting optimal trajectories have, at time t_4 , damped out all oscillations in $\Delta\dot{\delta}$ and $\Delta\delta$ and what remains is a damped exponential decay to the origin, as influenced by the pole at -13.3. Secondly, the search has been limited to a maximum of three possible switching instants. It is possible that with a greater number of switching instants a smaller value of T could be reached.

CHAPTER VI

CONCLUSIONS AND SUGGESTIONS FOR FURTHER STUDY

An iterative scheme for solving time optimal control problems has been presented, and applied to the problem of power system damping. The results indicate that for a mechanical torque input disturbance, the optimal control $u(t)$ will have two switching instants. Furthermore, as long as Figure 11 is followed, the two switching instants have constant values. However, use of Figure 11 will make practical implementation more difficult in that the control magnitude will have to be adjusted in accordance with the disturbance magnitude. As has been pointed out, a varying magnitude of control does not follow from Pontryagin's Principle and a possible explanation for this discrepancy has been given. Further research could involve verification of this explanation by solving the problem using some other form of iterative scheme. The switching curves in four dimensional state space, under a constant control magnitude, have also been presented. From these curves it is possible to generate a feedback control, which will predict the correct value of control $u(t)$ for the present values of the state variables.

In regard to the practical aspects of the results, further research is required. Due to the fact that there will be a delay in measurement of the disturbance magnitude, as

well as the fact that instantaneous switching is a practical impossibility, a sub - optimal system will definitely have to be used.

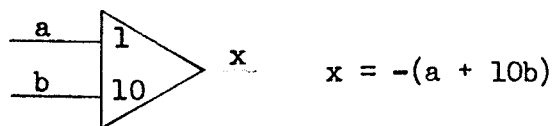
The iterative scheme has been designed for a time optimal solution as applied to the Heffron and Phillips plant. With slight modifications, any other plant can be substituted into the iterative scheme. Furthermore, all other optimal control problems, including cost optimal and fuel optimal problems can be very easily solved using the iterative scheme. As the EAI 580 hybrid computer is limited in size, larger problems will undoubtedly have to be solved on a digital computer.

APPENDIX A

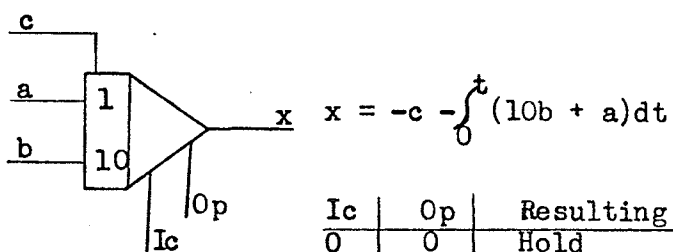
Computer Symbols

Logic 1 = High = +5volts
 0 = Low = 0volts

Summer
 (Inverter)

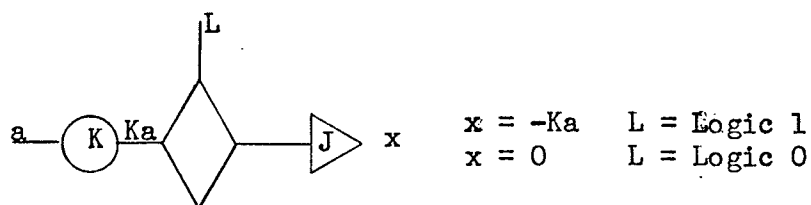


Integrator



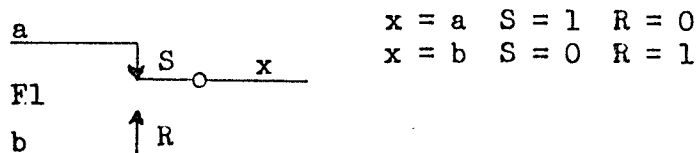
Ic	Op	Resulting mode
0	0	Hold
0	1	Operate
1	0	Initial Condition
1	1	Initial Condition

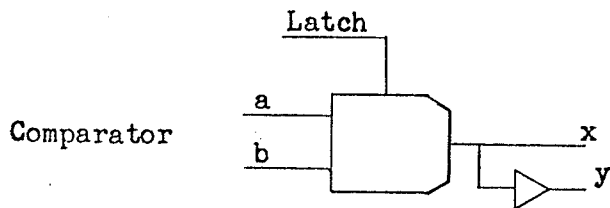
D-A Switch



Logic Signal F1

Function
 Switch

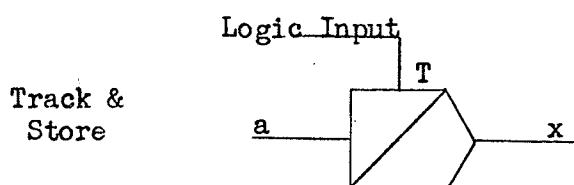




$$x = 1 \quad y = 0 \quad (a + b) > 0$$

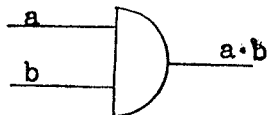
$$x = 0 \quad y = 1 \quad (a + b) < 0$$

When the Latch input is high, (Latch = 1), the comparator output is frozen (Latched); it cannot change, regardless of what the analog input does.



When the T input is at logic 1 the unit is in the Track mode and the output is minus the analog input ($x = -a$). When the T input is at logic 0 the unit is in the Store mode; its output is held constant, thus "remembering" the value it had at the instant of switching.

AND Gate



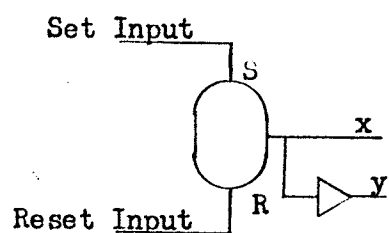
a	b	a · b
0	0	0
1	0	0
0	1	0
1	1	1

OR Gate



a	b	a + b
0	0	0
1	0	1
0	1	1
1	1	1

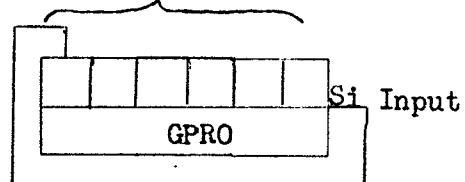
Flip Flop



S Input	R Input	x	y
0	0	Either 0 or 1	Either 0 or 1
0	1	0	1
1	0	1	0
1	1	Changes state	Changes state

Ring Shift Register

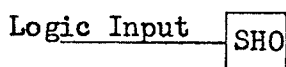
Individual FF Outputs



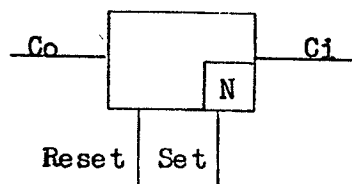
SHO is the control input.

SHO = 1 a shift occurs

SHO = 0 no shift occurs



Counter



If Set is high (logic 1), output

Co is high (logic 1). If Reset is

high, output Co is low (logic 0).

Ci is the input logic to the counter.

If Ci is high and the counter is

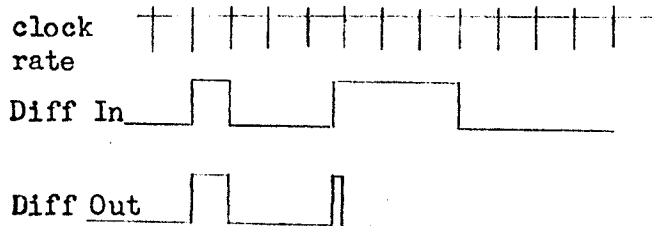
set, the counter will count up one

at every clock pulse. Once it has

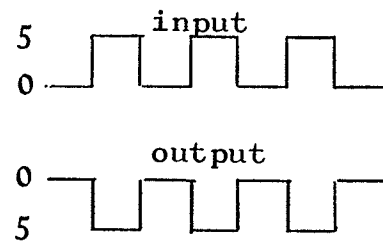
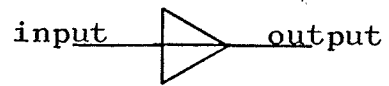
counted to $N + 1$, the output Co goes

low, and the counter is reset.

Differentiator



Digital
Inverter



Pot Settings

1. .127	12. .0100	23. R_{30}
2. 1.27 K_3	13. .0250	24. R_{40}
3. .127 K_4	14. .0100	25. .0200
4. .690	15. Variable	26. .0200
5. .605 K_2	16. Variable	27. .0200
6. .0605 K_1	17. Variable	28. .0200
7. -.1 K_5	18. Variable	29. .5600 U
8. K_6	19. .05n	30. .1 U
9. .0010	20. .10n	31. .0100
10. .605 N	21. R_{10}	32. .0100
11. .605 N	22. R_{20}	33. .0010

Initial Settings

H_2 — High

H_1 — Low

F01 — Set

Ex_1 — High

F04 — Set

F06 Set

Ex^+ — Low

Cntr. 1. — Set

Note: The signals A and \bar{A} , after the flip flop, were used to run the rest of the simulation. (see Figure 5)

On setting pot 29, the output voltage of the flip flop used as an input to the pot must be considered. The magnitude of the output voltage will vary with each flip flop.

BIBLIOGRAPHY

1. Athans, M. and P. L. Flab, Optimal Control
McGraw-Hill Book Co. 1966.
2. Bekey, G.A. and W.J. Karplus, Hybrid Computation
John Wiley and Sons Inc. 1968.
3. Demello, F.P. and C. Concordia., "Concepts of
Synchronous Machine Stability as Affected by
Excitation Control," I EEE Trans. on Power
Apparatus and Systems, Vol. PAS -88
No. 4, April 1969, pp. 316-329.
4. Eaton, J.H., "An Iterative Solution to Time Optimal
Control," Journal of Math. Analysis and App-
lications, Vol. 5, pp. 329-344, October 1962.
5. Fogarty, L.E. and R.M. Howe, "Trajectory Optimization
by a Direct Descent Process," Simulation,
Volume 11, No. 3, Sept. 1968, pp. 145-155.
6. Gilbert, E., "Hybrid Computer Solution of Time
Optimal Control Problems," AFIPS Conference
Proceedings, Volume 23, 1963, pp. 197-204.
7. Gilbert, E., "The Application of Hybrid Computers
to the Iterative Solution of Optimal Control
Problems," Computing Methods in Optimization
Problems, Balakrishnan and Neustadt, 1964,
pp. 261-284.
8. Grad, J. and M.A. Brebner, "Algorithm 343,
Eigenvalues and Eigenvectors of a Real General
Matrix," Communications of the A.C.M., Volume
11, Number 12, December 1968, pp. 820-826.
9. Hannauer, G., "Multiparameter Optimization," E.A.I.
Basics of Parallel Hybrid Computers, Appendix 6.
10. Heffron, W.G. and R.A. Phillips, "Effect of a Modern
Amplidyne Voltage Regulator on Under-excited
Operation of Large Turbine Generators," Trans.
A.I.E.E. Power Apparatus and Systems, Vol. 71,
Aug. 1952, pp. 692-697.
11. Hsu, J.C. and A.V. Meyer, Modern Control Principles
and Applications, McGraw-Hill Book Co. 1968.

12. Knudsen, H.K., "An Iterative Procedure for Computing Time - Optimal Controls," IEEE Trans. On A.C., January 1964, pp. 23-30.
13. Korn, G.A., "Enforcing Pontryagin's Maximum Principle by Continuous Steepest Descent," IEEE Trans. on Electronic Computers, Vol. EC-13, August 1964, pp. 475-476.
14. Korn, G.A. and H. Kosako, "A Proposed Hybrid-Computer Method for Functional Optimization," IEEE Trans. on Computers, Feb. 1970, pp. 149-153.
15. Maybach, R.L., "Solution of Optimal Control Problems on a High - Speed Hybrid Computer," Simulation, November 1966, pp. 238-245.
16. Moroz, A.I., "Synthesis of Time - Optimal Control for Linear Third - Order Systems," Automation and Remote Control, No. 5, May 1969, pp. 657-668.
17. Moroz, A.I., "Synthesis of Time - Optimal Control for Third - Order Linear Systems II," Automation and Remote Control, No. 7, July 1969, pp. 1032-1042.
18. Moroz, A.I., "Synthesis of Time - Optimal Control for Third - Order Linear Systems III," Automation and Remote Control, No. 9, Sept. 1969, pp. 1367-1376.
19. Neustadt, L.W., "Synthesizing Time Optimal Control Systems," Journal of Mathematical Analysis and Applications, Volume 1, No. 1-4, 1960, pp. 484-493.
20. Ryckman, G.W., "Bang-Bang Excitation Control of Power System Stability," M.Sc.EE. thesis, University of Manitoba, May 1970.
21. Smith, F.B., "Time Optimal Control of Higher Order Systems," I.R.E. Trans. on A.C., February 1961, pp. 16-21.
22. Wingrove, R.C. and J.S.Raby, "Trajectory Optimization Using Fast -Time Repetitive Computation," AFIPS Conference Proceedings, Volume 29, 1966, pp. 799-808.

23. Yastreboff, M., "Synthesis of Time - Optimal Control by Time Interval Adjustment," IEEE Trans. on A.C., December 1969, pp. 707-710.
24. Yu, Yao-Nan, Khien Vongsuriya, and Leonard N. Wedman, "Application of an Optimal Control Theory to a Power System," IEEE Trans. on Power Applications and Systems, Vol. PAS. -89, No. 1, Jan. 1970, pp. 55-62.